Solid Earth

Rift and plume: a discussion on active and passive rifting mechanisms in the Afro-Arabian rift based on synthesis of geophysical data

Ran Issachar[1,2]**, Peter Haas**[1,3]**, Nico Augustin**[3]**, and Jörg Ebbing**[1]

[1]Institute for Geosciences, Geophysics, Kiel University, Kiel, Germany
[2]Geological Survey of Israel, Jerusalem, Israel
[3]GEOMAR Helmholtz Centre for Ocean Research, Kiel, Germany

Correspondence: Ran Issachar (ranis@gsi.gov.il)

Abstract. The causal relationship between the activity of mantle plumes and continental break-up is still elusive. The Afro-Arabian rift system offers an opportunity to examine these relationships, in which an ongoing continental break-up intersects a large Cenozoic plume-related flood basalt series. In the Afar region, the Gulf of Aden, the Red Sea, and the Main Ethiopian Rift form an R-R-R triple junction within plume-related flood basalt series. We provide an up-to-date synthesis of the available geophysical and geological data from this region. We map the rift architecture in the intersection region by applying the difference in Gaussians to the topography and the bathymetry and interpreting vertical gravity gradients and Bouguer anomalies. With the aid of these methods we review the spatiotemporal constraints in the evolution of the different features of the plume–rift system.

Our results show rough and irregular morphologies of the Gulf of Aden and the Red Sea arms in contrast to the symmetric, continuous, and smooth Main Ethiopian Rift. The triple junction formed by the northeastward propagation of the Main Ethiopian Rift and developed simultaneously with the abandonment of the tectonic connection between the Red Sea and the Gulf of Aden through Bab al Mandab Strait. The triple junction was the last feature to develop in the plume–rift system and marked a tectonic reorganization. By this time, all rift arms were sufficiently evolved and the break-up between Africa and Arabia was already accomplished.

We argue that the classical active and passive rifting mechanisms cannot simply explain the progressive development of the Afro-Arabian rift. Instead, we propose a plume-induced

plate rotation, which includes an interaction between active and passive mechanisms. In this tectonic scenario, the arrival of the Afar plume provided a push force that promoted the rotation of Arabia around a nearby pole located to the northwest of the plate boundary, enabling the rifting and, ultimately, the break-up of Arabia from Africa.

1 Introduction

The causal dependency between the eruption of flood basalts and continental break-up is still unclear, although a close occurrence between these two phenomena has been recognized for a long time. Continental flood basalts, often referred to as traps, form large igneous provinces covering huge continental areas (Bryan and Ferrari, 2013; Ernst, 2014). Continental flood basalts are often associated with extensive volcanism during short time intervals, which are brought to the surface by deep-seated mantle plumes (Richards et al., 1989; White and McKenzie, 1995; Koppers et al., 2021), although other mechanisms were also suggested (e.g., Anderson, 1994, 2005). There is evidence for a close temporal and spatial occurrence between the eruption of flood basalts and continental break-up. In particular, when reconstructed back to their original plate tectonic configuration, an R-R-R triple junction is typically found within the flood basalt areas (Morgan, 1971; Burke and Dewey, 1973; Buiter and Torsvik, 2014). Using the geological record to examine the mutual dependency of these processes is challenging. It requires high

precision in the temporal and spatial development of the volcanic and tectonic features, often obscured by the overprint of different tectonic processes.

The Afar region in the central parts of the Afro-Arabian rift system is recognized as a key locality to examine models of plume–rift association, offering a young and active case study in which a plume, regional uplift, an R-R-R triple junction, break-up, and oceanic spreading co-exist and are superimposed (Fig. 1). Plume–rift association is mainly explained as either "active" (e.g., Sengör and Burke, 1978) or "passive" (e.g., White and McKenzie, 1989), with no interaction between those mechanisms. Despite the contrary implications, the Afar case study was used as a prime example to support both the active (e.g., Burke and Dewey, 1973) and the passive (e.g., White and McKenzie, 1989) mechanisms, and some authors argued that both processes are required to explain the observations (e.g., Courtillot et al., 1999). The discrepancy can be primarily attributed to the lack of accurate geological and geophysical evidence regarding the uplift, volcanism, and rifting phases. Moreover, studies show that changes in plate motions and the activity of plumes occurred concurrently, suggesting new concepts in which plumes cause rapid deviations in the kinematics of nearby plates (e.g., Cande and Stegman, 2011).

The purpose of this paper is to discuss the causal relationship between the Afar plume and rifting along the Afro-Arabian rift system in light of the large amounts of data collected in recent years and the new concepts derived from studies of the Indian plate. For this, we first review the timing of volcanism and uplifts in Ethiopia and Yemen and the timing of rifting along the Gulf of Aden, the Red Sea, and the Main Ethiopian Rift. We further provide an analysis and interpretation of modern geophysical datasets, including topography, bathymetry, and gravity, and incorporate the distribution of offshore magnetic anomalies, earthquakes (ML > 4), and onshore Quaternary volcanos. Using these datasets, we map the architecture of the rifts and describe the development of rift segments. Finally, we compare our results with recent models and other case studies in the world, aiming to shed light on the causal relationship between mantle plumes and tectonic processes.

2   Active and passive mechanisms for plume–rift association

The existence of deep mantle convection and its interaction with the Earth's lithosphere was already pointed out by Wilson (1963), and a close occurrence to continental break-up was soon noticed by the abundance of hot spots near many rift junctions (Morgan, 1971) and flood basalt volcanism along passive margins (Richards et al., 1989). Although Morgan (1971) speculated that deep mantle convection has a significant role in accelerating the overlying tectonic plates, it was later realized that slab pull provides the main driving
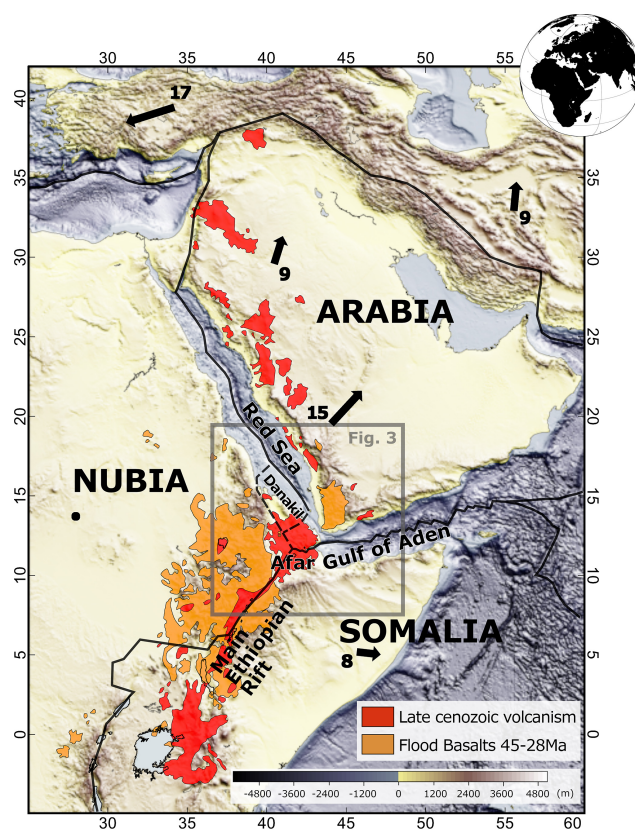

Figure 1. Elevation map of the study area, showing the general plate tectonic configuration (from USGS and from Viltres et al., 2020, in the Afar region) and Cenozoic volcanics (modified from Varet, 1975; Davison et al., 1994; Beyene and Abdelsalam, 2005; Bosworth and Stockli, 2016). Black arrows indicate GPS velocities with respect to Nubia (modified from Reilinger et al., 2006).

force for plate motion (Forsyth and Uyeda, 1975). In their landmark paper, Burke and Dewey (1973) presented 45 case studies of rift junctions associated with hot spots. They proposed a model in which plume-associated uplift and volcanism precede and generate the rift arms, initiated from a triple junction within the plume region. Afar was used as a first and prime example, highlighting its importance as a young and active case study; however, they already noted a complex distribution of continental fragments and magnetic anomalies (Burke and Dewey, 1973).

Following these insights, active rifting models were developed to explain plume–rift associations (e.g., Keen, 1985; Moretti and Froidevaux, 1986; Campbell and Griffiths, 1990; Hill, 1991; White and McKenzie, 1995). These models generally propose that rifting can result from a combination of processes derived from the actively rising head of an anomalously hot mantle. These mantle plumes impinge on and erode the base of the lithosphere, which prompt uplift and decompression melting, introduce internal extensional forces, and ultimately lead to break-up. Accordingly, regional uplift
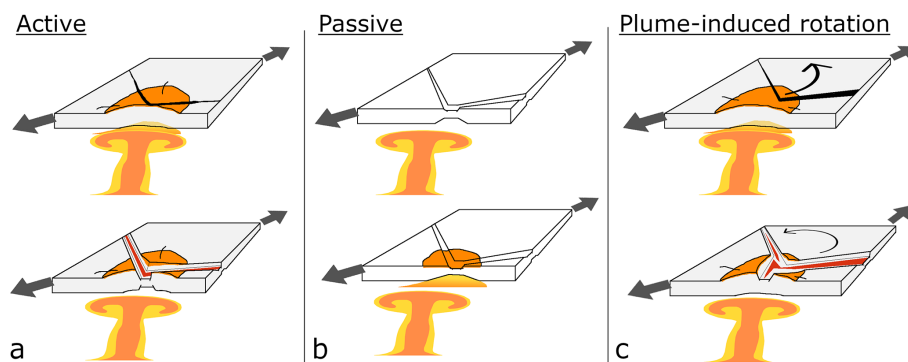
Figure 2. Schematic mechanisms for plume–rift association in the Afro-Arabian rift. **(a)** Active mechanism (e.g., Campbell and Griffiths, 1990). The plume head impinges on and erodes the base of the lithosphere, which prompts uplift and decompression melting. This introduces internal extensional forces at the crust, leading to break-up. **(b)** Passive mechanism (e.g., White and McKenzie, 1989). Rifting is initiated solely by the remote stresses, regardless of the underlying plume. In this mechanism, the production of massive volcanism is allowed when the thinned and stretched lithosphere is underlaid by the thermal anomaly in the mantle. Flood basalt volcanism is generated by decompression melting of the passively rising hot asthenospheric mantle. **(c)** Plume-induced plate rotation (van Hinsbergen et al., 2021). Plume push forces sourced by the drag of the flowing asthenosphere add up to the remote stresses to change the plate kinematics. In this mechanism flood basalt volcanism is actively controlled; however, rifting is triggered by the new plate kinematics.

and volcanism are expected to precede rifting, which would initiate from a triple junction above the mantle plume head (Fig. 2a).

Later contributions challenged the active view, arguing that a passive asthenospheric upwelling can also resolve the occurrence of flood basalt near rifts (firstly introduced by White and McKenzie, 1989). In this view, rifting is initiated by the remote extensional stresses, usually along former sutures and weak zones, regardless of underlying plumes. The production of massive volcanism is allowed when the thinned and stretched lithosphere is underlaid by a thermal anomaly in the mantle. The volcanism is generated by decompression melting of the hot asthenospheric mantle, which passively rises. As plumes form large areas of high temperatures in the mantle, massive volcanism is found on Earth's crust close to rifts. Accordingly, subsidence is a precondition required for magmatism, and there is no triggering mechanisms for a triple junction to form within the flood basalt region (Fig. 2b).

Although active and passive mechanisms have been discussed in the last 50 years, the role of plumes in initiating rifting is still unclear and much debated. Even for well-studied and prime examples of plume–rift association such as the Siberian, Parana–Etendeka, Deccan, and Greenland traps, there is no agreement on whether active processes initiated rifting (Geoffroy, 2005; Ivanov et al., 2015; Frizon De Lamotte et al., 2015; Fromm et al., 2015; Mitra et al., 2017). Some authors emphasize the significance of pre-existing lithosphere weaknesses along former sutures and structures (Buiter and Torsvik, 2014; Will and Frimmel, 2018), while others show the potential of plumes to thermally and chemically erode the base of the lithosphere in the weakening process allowing rifting (Sobolev et al., 2011). Additionally,

some models demonstrate that mixed active–passive scenarios can better explain observation (Koptev et al., 2018) and even that both mechanisms are needed to explain temporal variations in rifts (Huismans et al., 2001).

In addition to the dichotomic views, a complex relationship in which plumes can influence the horizontal velocities of plates is suggested based on detailed plate reconstructions and numerical modeling (van Hinsbergen et al., 2011, 2021; Cande and Stegman, 2011; Chatterjee et al., 2013; Pusok and Stegman, 2020). In these studies, an abrupt change in plate velocities is correlated with the arrival of a nearby plume head. In the kinematic record of the Indian plate, the arrival of the Marion and Reunion plumes (associated with the Morondava and Deccan LIPs) is synchronized with an abrupt plate speed-up and an Euler pole shifting. During the arrival of the Reunion plume (at ~ 65 Ma), the acceleration of the Indian plate was coupled with transitory slowing of the African plate (Cande and Stegman, 2011). Plume push forces, sourced by the drag of the flowing asthenosphere, were shown to be capable of changing the kinematics of nearby plates and even triggering the formation of new plate boundaries through a mechanism termed plume-induced plate rotation (van Hinsbergen et al., 2021) (Fig. 2c).

3   Geological setting

The Afro-Arabian rift system extends from Turkey to Mozambique (McConnell and Baker, 1970) and is the current episode of the Phanerozoic break-up of the East African continental plate (Bosworth, 2015). It contains rifting in the Gulf of Aden, in the Red Sea, and in East Africa. In the center of that system, the Ethiopian northwestern and south-eastern plateaus represent an elevated topography with the
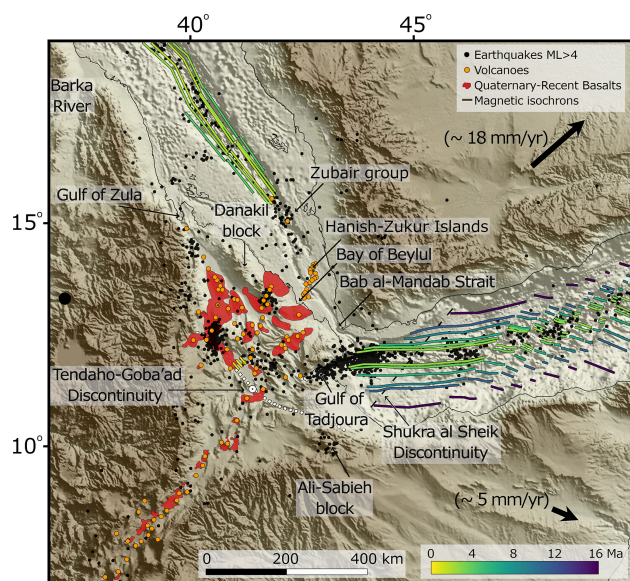
Figure 3. Map of the Afar region showing magnetic isochrons (modified from Fournier et al., 2010; Bridges et al., 2012; Schettino et al., 2016), earthquake locations (from the ISC catalog), Holocene onshore volcano locations (from GVP catalog and Viltres et al., 2020), and recent volcanism (modified from Keir et al., 2013).

highest peak of 4620 m (Ras Dashan) and an average elevation of 2000 m a.s.l. (above sea level). This area is part of the so-called African Superswell, a wide region of anomalously high topography comprising East Africa (Lithgow-Bertelloni and Silver, 1998; Corti, 2009). In western Yemen, the Sarawat Mountains are the highest peaks in the Arabian Peninsula, reaching more than 3000 m, only 100 km away from the shoreline of the Red Sea. These mountains show a typical stair morphology with steep slopes at the western and southern sides, while the eastern shows gentler downward slopes.

The Gulf of Aden is the most developed rift segment in the Afro-Arabian rift, with a mature and fully developed oceanic spreading center connected to the mid-ocean ridge in the Indian Ocean. Six pairs of magnetic anomalies associated with seafloor spreading are recognized along the Gulf of Aden (Fournier et al., 2010) (Fig. 3). Oblique rifting and high-angle structural inheritance along the Gulf of Aden resulted in multiple ridge segments and fracture zones (i.e., transform faults; Leroy et al., 2013; Autin et al., 2013; Bellahsen et al., 2013; Duclaux et al., 2020).

At the northern parts, the rifting in the Red Sea is connected by the Dead Sea Fault to the Eurasian collision zone along the Taurus–Zagros Mountains. The Red Sea is experiencing the last stages of break-up and early stages of oceanic accretion. An oceanic spreading center with three pairs of ridge-parallel magnetic anomalies is recognized in the southern parts of the Red Sea (Schettino et al., 2016) (Fig. 3).

However, oceanic crust is probably flooring most of the basin (Augustin et al., 2021).

The Main Ethiopian Rift is the northernmost section of the intra-continental rifting in East Africa, splitting the not-yet well-individualized Somali plate from Africa (Chorowicz, 2005). Active rifting in the Main Ethiopian Rift is characterized by a narrow rift valley, in which volcanic and tectonic activities are localized and influenced by oblique rifting (Corti, 2009).

The abovementioned three rift arms meet in the Afar triangle (Fig. 3). It is a low-elevation area compared to the high Ethiopian plateaus and thus commonly referred to as the Afar "depression". Nevertheless, this term is misleading as the Afar triangle is included within the rifted area and is geologically elevated from the deep bathymetry of the Gulf of Aden and the Red Sea basins. The Afar triangle is mainly floored by Pliocene and younger volcanic rocks, where Miocene volcanic series are exposed along the western margins and at the elevated Danakil block. It comprises many volcanoes and axial volcanic ranges (Fig. 2), where the northeastern side is characterized by transverse volcanic fields and the southwestern side by central volcanoes (Varet, 2018). Two symmetric magnetic anomalies have been recognized in the Tendaho graben, similar to those observed along spreading centers in the Gulf of Aden (Bridges et al., 2012). These could be associated with either young oceanization or linear anomalies developed in transitional crust (Ebinger et al., 2017). Structurally, several mega-scale accommodation zones connect the rift segments, and the location of a main triple junction is recognized at $11.0°$ N, $41.6°$ E along the Tendaho-Goba'ad discontinuity (e.g., Tesfaye et al., 2003) (Fig. 3).

4 Temporal constraints

4.1 Flood basalts and uplift

Vast efforts were made to study the chemistry and chronology of flood basalts in East Africa (see review by Rooney, 2017). Two phases of extensive flood basalt volcanism are associated with plume–lithosphere interaction (Fig. 4). The early phase is mainly confined to southern Ethiopia and northern Kenya. The timing of this event is poorly constrained to 45–35 Ma (George et al., 1998). The second phase of flood basalt eruptions was more voluminous, more widespread, and shorter-lived. The earliest basalts of this phase date back to 34 Ma near the Tana Basin in Ethiopia (Prave et al., 2016) and 31 Ma in western Yemen (Peate et al., 2005) (Fig. 4). The traps accumulated very rapidly, in less than 6 Ma (Coulié et al., 2003), and include tholeiitic to alkaline compositions of asthenosphere mantle source (Mattash et al., 2013). Thick sequences of up to 2 km are observed within a widespread region in Ethiopia and Kenya (Bellieni et al., 1981; Wescott et al., 1999; McDougall and
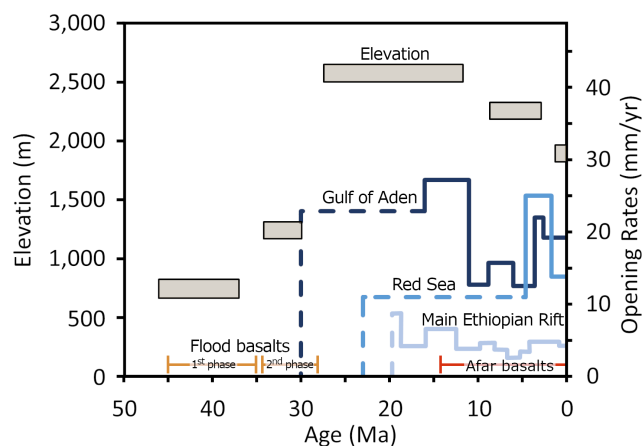
Figure 4. Elevation of the Ethiopian–Yemen plateau (gray boxes, after Sembroni et al., 2016; Faccenna et al., 2019), volcanic episodes (orange and red bars), and opening rates of the rift arms (blue lines, modified from Fournier et al., 2010; DeMets and Merkouriev, 2016; Schettino et al., 2018). Dashed lines indicate estimations from geological observations and solid lines from magnetic anomalies.

Brown, 2009). It is commonly accepted that these flood basalts are of deep-seated mantle plume origin (Koppers et al., 2021). However, the formation mechanism is debatable and may involve multiple plume impingements within a broad upwelling zone connected to the African superplume in the lower mantle (Meshesha and Shinjo, 2008) or a single plume–lithosphere interaction (Rooney, 2017).

An elevated topography is associated with the eruption of the flood basalts in Ethiopia. The flood basalts are almost exclusively positioned within the elevated regions of the Ethiopian and Somali plateaus and the Sarawat Mountains in southwest Yemen (Fig. 1). The dynamic topography component supports up to 1 km of present-day elevation of the Ethiopian and Somali plateaus, supporting the significant contribution of mantle convection to the regional uplift (Gvirtzman et al., 2016). Although the uplift chronology is not easily resolved, recent studies infer it is a long-term feature already active before the emplacement of the flood basalts (Sembroni et al., 2016; Faccenna et al., 2019). Regional uplift is estimated to have begun before 40 Ma, with maximal uplifts between 12 and 28 Ma, reaching an average elevation of 2500 m (Fig. 4) (Sembroni et al., 2016).

4.2   Gulf of Aden

The beginning of continental rifting in the Gulf of Aden relies on the dating of sedimentary sequences, published in the 1990s (see Bosworth et al., 2005, for a review). Onshore outcrops in Yemen (Watchorn et al., 1998) and in Oman (Roger et al., 1989) and offshore wells (Hughes et al., 1991), suggest that rifting in the central and eastern Gulf of Aden began in the early to mid-Oligocene, within the Rupelian

(33.9–27.8 Ma). Syn-rift sediments from the central Yemeni margins indicate that rift flank uplift occurred before any significant regional extension. The climax of continental rifting is estimated between 20 and 18 Ma (Watchorn et al., 1998). Radiometric dating indicates that the margins had already become stable in the early Miocene (Bosworth et al., 2005), and rift-to-drift transition is interpreted to have occurred between $\sim$ 21.1 and $\sim$ 17.4 Ma (Watchorn et al., 1998). The seafloor spreading center in the Gulf of Aden is recognized along most of its length and is connected to the mid-ocean ridge in the Indian Ocean through the Sheba Ridge (Gillard et al., 2021). In the central Gulf of Aden, magnetic isochrons suggest opening rates of $\sim$ 27 mm a^{-1} prior to 11 Ma and a slowdown after 11 Ma (Fig. 4). Chron 5C (purple stripes in Fig. 3; 16.0 Ma) is present along the Gulf of Aden up to the Shukra al Sheik discontinuity (Fig. 3; Fournier et al., 2010). This implies that the spreading center developed very rapidly, spreading over more than 700 km in less than 1.5 Myr. This fast propagation ceased at the Shukra al Sheik discontinuity. The youngest magnetic isochrons (2A, 2.6 Ma) are recognized up to 43.9° E in the eastern Gulf of Tadjoura, $\sim$ 150 km west to the Shukra al Sheik discontinuity, indicating that along this segment, the ridge propagated westward at an average rate of $\sim$ 11 mm a^{-1} in the last 16 Myr. Within the Gulf of Tadjoura, no direct evidence of oceanic spreading was reported in the literature.

4.3   Red Sea

Sedimentary sequences from offshore drillings suggest that rifting in the Red Sea postdated the rifting in the Gulf of Aden by a few million years (Bosworth et al., 2005). Independent studies suggest that rifting began simultaneously along the entire Red Sea in the late Oligocene–early Miocene at $\sim$ 23 Ma (Plaziat et al., 1998; Szymanski et al., 2016; Stockli and Bosworth, 2018; Morag et al., 2019). Magnetic isochrons associated with seafloor spreading are recognized at the southern parts of the Red Sea (Fig. 3; Girdler and Styles, 1974). However, oceanic lithosphere is probably abundant along most of the basin (Augustin et al., 2021). Chron 3 (4.2 Ma) is only present between 16 and 18° N, while chrons 2A (2.6 Ma) and 2 (1.8 Ma) are present up to 22° N (Schettino et al., 2016). The recognition of chron 5 (10 Ma) in the central Red Sea was recently suggested to mark the beginning of seafloor spreading (Okwokwo et al., 2022). Structural reconstructions, geodetic measurements, and magnetic anomalies suggest an opening rate of $\sim$ 11 mm a^{-1} up to $\sim$ 4.6 Ma, an abrupt increase in the opening rate to $\sim$ 25 mm a^{-1} between 4.6 and 1.8 Ma, and a decrease to $\sim$ 14 mm a^{-1} (Fig. 4; Schettino et al., 2018). The southern edges of the magnetic chrons suggest that the southern Red Sea ridge propagated 50 km southwards between 4.2 and 2.6 Ma ($\sim$ 30 mm a^{-1}). Since 2.6 Ma, the Red Sea ridge has not propagated southward, probably due to the

decrease in angular velocity of Danakil relative to Arabia (Fig. 3; Schettino et al., 2018).

4.4   Main Ethiopian Rift

Age of faulting and volcanism along segments of the Main Ethiopian Rift suggest a diachronous development of the different segments of the Main Ethiopian Rift (e.g., Bonini et al., 2005). However, there is no agreement regarding the exact timing of events and even the propagation trend of the rift. Reconstructions based on magnetic anomalies from the southwestern Indian ridge suggest an upper limit for the Nubia–Somalia separation at ~ 19 Ma, including large uncertainties regarding the rates and directions of the relative motion pre-16 Ma (DeMets and Merkouriev, 2016) (Fig. 4). Geochronological data suggest that volcanism and rifting in East Africa started at the Turkana depression in southern Ethiopia at 50 Ma (Varet, 2018) and episodically propagated northwards. However, it is still a matter of debate if there is a general propagation pattern or if different segments propagated in different directions (see Figs. 42–44 in Corti, 2009). Nevertheless, radiometric dating of structural features indicates that extension commenced at ~ 11 Ma within the northern Main Ethiopian Rift (Wolfenden et al., 2004).

In summary, regional uplift and flood basalt volcanism in Ethiopia preceded the rifting of the Afro-Arabian rift (e.g., Rooney, 2017). The rift arms developed diachronically, with the onset of rifting in the eastern Gulf of Aden occurring during the late phases of flood basalt volcanism (at ~ 30 Ma), whereas rifting in the Red Sea (at ~ 23 Ma) and the Main Ethiopian Rift (at ~ 19 Ma) lagged by ~ 5–7 Myr.

5   Data and methods

We used bathymetry (GEBCO compilation) and topography (SRTM 15+) data to identify morphotectonic features. To highlight and map the architecture of the margins and axes of the rifts, we applied the difference of Gaussians (Fig. 5) method to the topography and the bathymetry grids (Akram et al., 2017). This method allows a fast and accurate edge detection of elevation using active spatial bandpass filtering. We applied luminance coloring to the resulting grid using the open-source image processing software Gimp.org.

To study density-related shallow crustal structures, we used the satellite-altimetry-derived vertical gravity gradient (VGG) model of Sandwell et al. (2014), offering 1 arcmin resolution at offshore regions. As higher frequencies are intensified in the spectral power of the VGG, its anomalies are more source-localized and shallow-sensitive than free-air anomalies. To enhance the edges associated with the VGG, we applied a linear 11-color color map, further applied transparency to the VGG map, and projected it on a shaded relief (Fig. 6a).

To study deeper crustal structures and eliminate the topography effect, we used the Bouguer gravity anomaly (BGA), derived from the XGM2019 gravity model (Zingerle et al., 2020) and calculated with a grid step of 0.1°. The XGM2019 is the most updated global gravity model of the International Centre for Global Earth Models (ICGEM) and is provided in terms of spherical harmonics up to 2159° (Ince et al., 2019; Zingerle et al., 2020). In addition, we applied a linear 240-color color map to enhance BGA structures, further applied transparency to the BGA map, and projected it on a shaded relief (Fig. 6b).

To better correlate and discriminate crustal structures and rift features, we considered 1913 earthquake locations (Fig. 3) from the International Seismological Centre catalog with minimum magnitudes $> 4 \, M_L$, recorded between 1964 and 2019. To better infer recent tectonic and volcanic activity, we further considered the locations of Quaternary onshore volcanoes (Fig. 3) from the Global Volcanism Program (Smithsonian Institution) and Google Earth mapping.

6   Results

6.1   Rift margins

The most prominent morphological feature of the rift system is the escarpment along its shoulders. The escarpments mark the rift margin as they distinguish between (1) uplifted pre-rift rocks of the Arabian–Nubian shield or trap basalt sequences and (2) Quaternary arid fluvial sediments or young volcanic sequences, although several continental crustal fragments are present within the Afar triangle. The edge detection analysis of topography and bathymetry data allows us to outline the rift margins (Fig. 5). This method highlights high-frequency details. Steep gradients are shown in bright colors and moderate gradients in gray (Fig. 5).

In the Red Sea, the escarpments are generally continuous with an average rift width of 440 ± 20 km (calculated perpendicular to the Red Sea axis in the study area) and a general increase in rift width from north to south (Fig. 5b). We identify two segments that mark an abrupt change in rift orientation and rift width: (1) below 15.5° N on the African margin and 18° N on the Arabian margin (segment I in Fig. 5), the escarpment deviates from its general position parallel to the Red Sea trend, bending towards the Afar region. The escarpment is characterized by seismic activity from that point on the African side, which is also considered the northern point of the western Afar margins (Zwaan et al., 2020a). (2) Below 12.5° N on the African margin and 15° N on the Arabian margin (segment II in Fig. 5), we identify another abrupt change in both the orientation and the width of the rift. That point on the African margin is the intersection of the Tendaho-Goba'ad discontinuity and the western Afar margins (Tesfaye et al., 2003). We note that these changes are noticeable and similar on the African and Arabian sides (Fig. 5a).
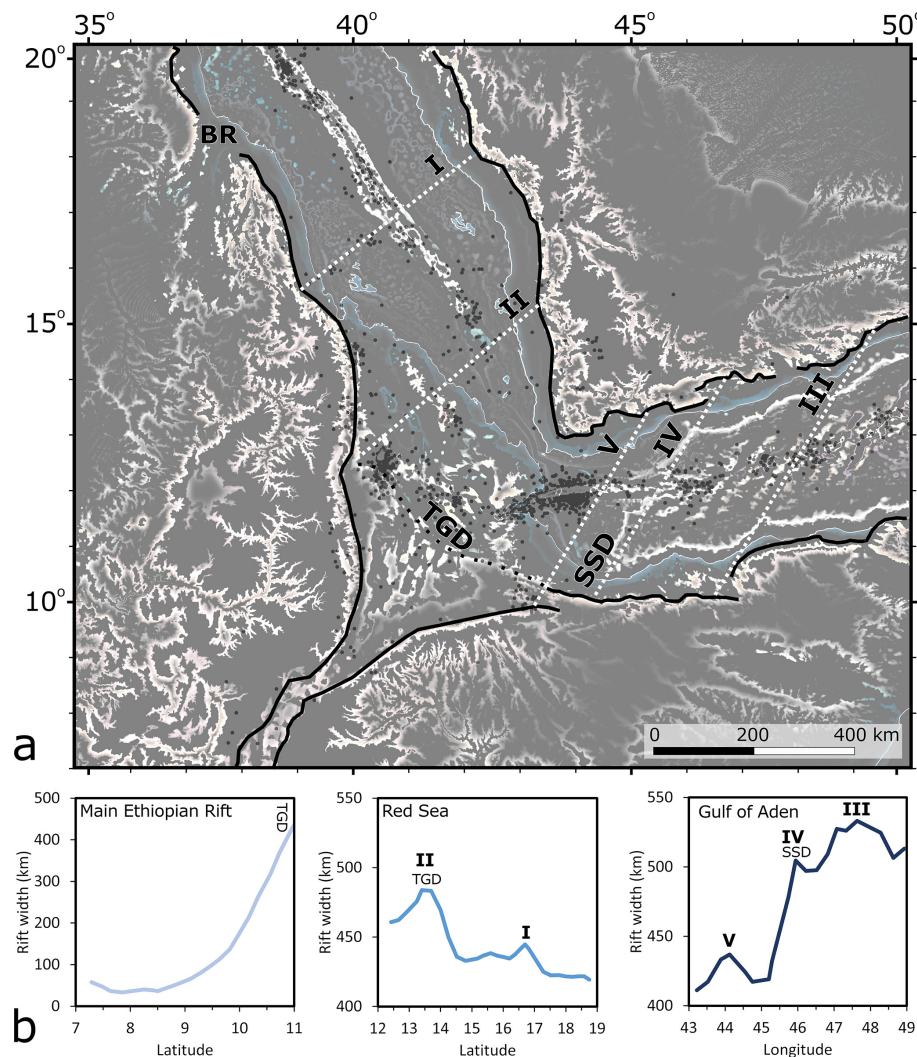
Figure 5. (a) Difference of Gaussians applied to topography and bathymetry showing rift margins (black lines). Dashed white lines indicate peaks in rift width. TGD is the Tendaho-Goba'ad discontinuity. SSD is the Shukra al Sheik discontinuity. Black dots indicate earthquake locations (ISC catalog). **(b)** Rift widths, calculated in rift-perpendicular directions.

In the Gulf of Aden, the escarpments generally follow the trend of the basin (Fig. 5). In the western parts, the escarpments are irregular and less continuous than those of the Red Sea and generally reflect the sinistral basin structures. This morphology is well explained by oblique rifting along the Gulf of Aden (Leroy et al., 2013). The average rift width in the study area is 470 ± 45 km (calculated rift-perpendicular), with a general eastward increase (565 km at 47.5° E and 420 km at 43.2° E; Fig. 5b). We recognize an abrupt change in rift width along three lines (III–V in Fig. 5), which are associated with fracture zones. Along the Somali margin, prominent sinistral offsets are recognized along lines III and V. This escarpment segment is a morphological continuation of the Tendaho-Goba'ad discontinuity lineament and is also prominent in the VGG map (Fig. 6a).

Although recognizable in the processed topography map, the rift shoulders are gentler in the Main Ethiopian Rift (Fig. 5a). They are prominent in the gravity data as they are associated with VGG and BGA highs (see profile A in Fig. 9). In the Afar region, the margins show a funnel shape (Fig. 5a). The distance between the Somali and Ethiopian escarpments steadily and monotonically increases from the Main Ethiopian Rift to the Tendaho-Goba'ad discontinuity (Fig. 5b), suggesting that this segment is intact and non-disturbed by the other arms of the rift system.

In summary, the rift margins of the Red Sea and the Gulf of Aden are interrupted within the vicinity of the Afar triangle, whereas the margins of the Main Ethiopian Rift smoothly funnel into the Afar triangle.
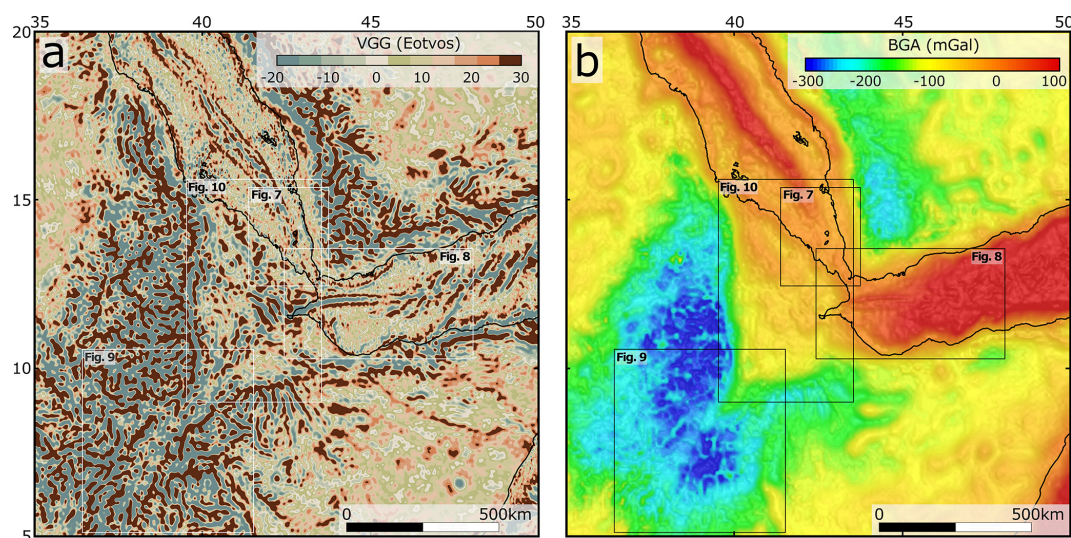
Figure 6. Gravity data for the Afar region. **(a)** Vertical gravity gradient from Sandwell et al. (2014). Bouguer anomaly model from ICGEM, XGM2019e (Zingerle et al., 2020).

6.2 Rift axes

Along the Red Sea and the Gulf of Aden basins, the rift axes are distinctively characterized by deep and sharp bathymetric troughs, VGG lows, BGA highs, and intense seismic activity (Figs. 3 and 6). However, with proximity to the Afar region, the rift axes change their characteristics.

The rift axis along the Red Sea is outlined by a deep and wide axial trough that ends at 14.5° N, approximately 400 km from the triple junction (Fig. 7a). South of 14.5° N, we find geophysical evidence that the rift axis is bent westwards, running onshore at the Bay of Beylul (white dashed line in Fig. 7b). The VGG signature and the bathymetry display highs along the walls (50 eotvos; eotvos $= 10^{-9}\,\mathrm{s}^{-2}$) and lows along the center (Fig. 7b and profile B). A trail of volcanic islands follows this path (Zukur–Hanish islands; Fig. 3), and the alignments of volcanic cones and vents on the islands are orthogonal to the trail of the islands (Mitchell and Bosworth, 2023; Gass et al., 1973). A general trend of recent magmatic bodies onshore meets this line at the Bay of Beylul (Fig. 3). However, major fault sets are not observed in the onshore area of Beylul (Rime et al., 2023). In addition, a best-fit GPS-based rigid block model suggests a block boundary along this path (Viltres et al., 2020), which is also supported by the fact that the rotation of Danakil relative to Arabia stopped around ~ 0.3 Ma (following Schettino et al., 2018, and Antonio Schettino, personal communication, 2024). In addition to the bent axial segment, a typical gravity signature of the Red Sea rift axis, with a 20 mGal central BGA peak and 60–40 eotvos VGG side peaks, is also recognized along the connection of the Red Sea with the Gulf of Aden at Bab al Mandab Strait (13.2 to 12.3° N; Fig. 7 profile CC'). Nevertheless, no earthquakes, volcanic activity, or faulted morphology are observed along this segment,

and thus we propose that this segment is not an active rift axis. However, diluted activity is inferred from the low and oblique velocity of Arabia in this area (Fig. 3).

In the Gulf of Aden, there is also a distinct change in the characteristics of the rift axis, approximately 400 km east to the triple-junction region (Fig. 8). East to the Shukra al Sheik discontinuity, the Gulf of Aden is a > 2000 m deep basin, which steeply deeps close to the shoreline. Along the basin, the axial trough is fragmented by oblique left-lateral transform faults (Fig. 3). On the other hand, west to the Shukra al Sheik discontinuity the basin is shallow (~ -700 m). In this section of the Gulf of Aden, the ~ 1700 m deep and ~ 400 km long curved axial trough impales the Afar triangle at the Gulf of Tadjoura (Djibouti) (Fig. 8). This axial segment has a distinct gravity signature with a 75 mGal central BGA peak and 20–35 eotvos VGG side peaks, and it is characterized by the most intensive seismic activity in the rift system, with over 1000 recorded events with magnitudes $> 4\,M_\mathrm{L}$ (ISC catalog; Ruch et al., 2021).

In the Main Ethiopian Rift, there are no abrupt changes in the morphology and trend of the rift valley in proximity to the Afar triangle (Fig. 9). Instead, the rift valley goes through an elevated dome peaking approximately 400 km from the triple junction (Fig. 9a). The along-strike profile (profile B in Fig. 9) shows that the rift valley reaches elevations of $<$ 2000 m and is associated with a BGA low of -220 mGal.

In the Afar triangle, the morphology and VGG data indicate two distinguished regions of axial segments (Fig. 10). (1) Southwest of the Tendaho-Goba'ad discontinuity, a NE-trending valley follows the NE trend of the Main Ethiopian Rift, characterized by distinct central volcanoes along the axial depression (Figs. 3 and 10a). (2) Northeast of the Tendaho-Goba'ad discontinuity, axial segments are com-
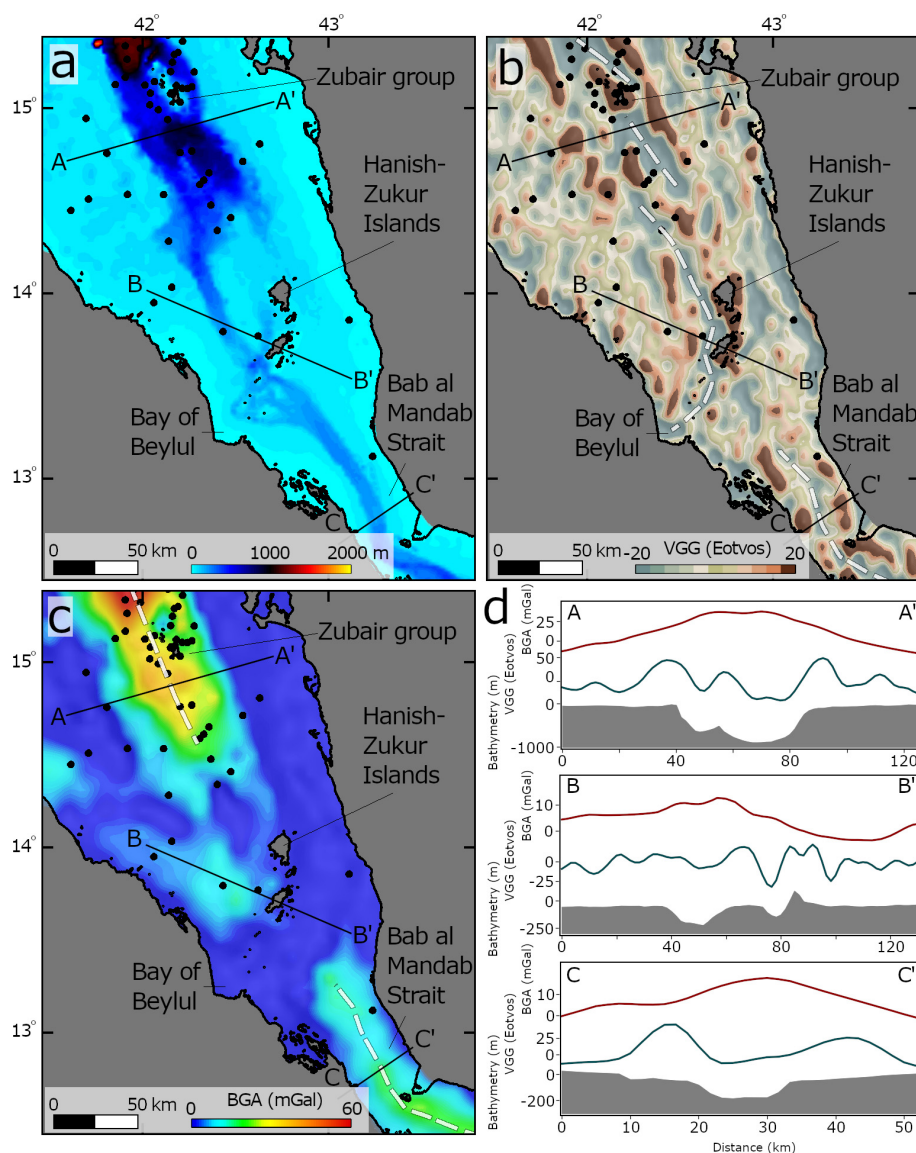
Figure 7. Bathymetry **(a)**, vertical gravity gradient **(b)**, and Bouguer anomaly **(c)** in the southern Red Sea. Black dots indicate earthquake locations (ISC catalog). **(d)** Profiles across rift axis.

posed of NW-trending short segments along volcanic ranges, parallel to the trend of the Red Sea.

In summary, the rift axes of the Red Sea and the Gulf Aden drastically change their trend and morphological characteristics ~ 400 km from the triple junction. In contrast, the trend and morphological characteristics of the Main Ethiopian Rift are consistent from the Ethiopian highs up to the triple-junction point in Afar.

7   Discussion

7.1   The architecture of the intersection region

The Afar triangle is the intersection region of three rift arms: the Gulf of Aden, the Red Sea, and the Main Ethiopian Rift. Far from the intersection region, the architecture of the rifts, with rift margins parallel to rift axes, suggests that rigid plate tectonics of the Nubian, Arabian, and Somali plates controlled their structural development (Garfunkel and Beyth, 2006; Reilinger et al., 2006; Reilinger and McClusky, 2011; Schettino et al., 2018). However, the architecture of the intersection region is not simply resolved by rigid plate kinematics (Garfunkel and Beyth, 2006). Our analysis points
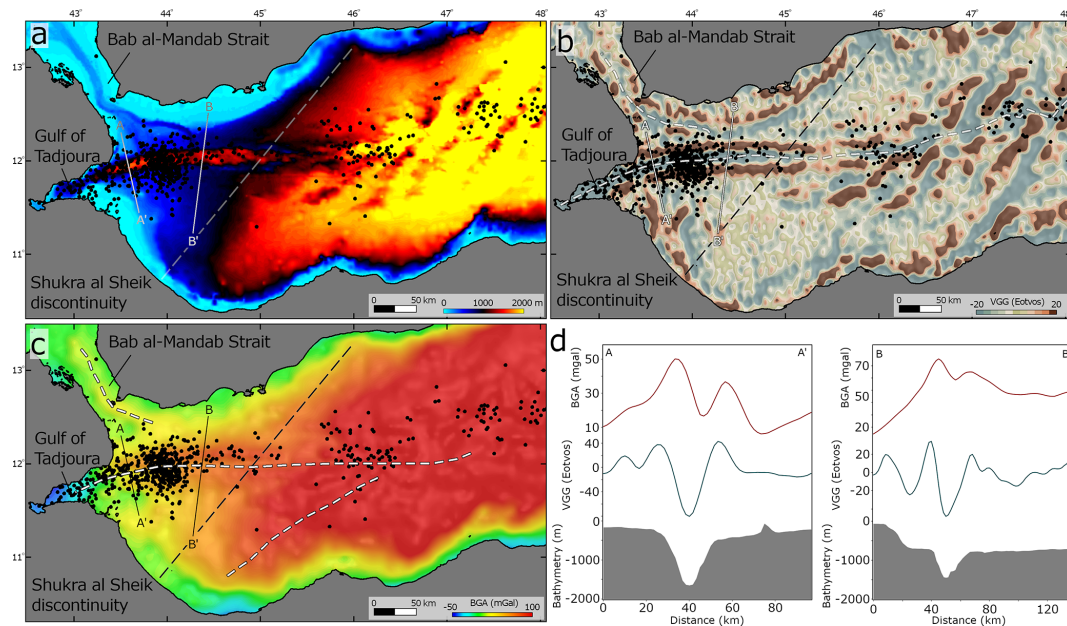
Figure 8. Bathymetry **(a)**, vertical gravity gradient **(b)**, and Bouguer anomaly **(c)** in the western Gulf of Aden. Black dots indicate earthquake locations (ISC catalog). **(d)** Profiles across rift axis.

to abrupt changes in the architectures of the Gulf of Aden and of the Red Sea rifts, ∼ 400 km from the triple junction. Here, the margins deviate from their general orientation, show peaks in rift width (segments I to V in Fig. 5), and are not parallel to the rift axes. The axes themselves deflect from their usual rift-parallel orientation and are curved towards the direction of the triple junction as they meet the shoreline, forming bays (Figs. 7 and 8). Within the Afar triangle, northeast of the Tendaho-Goba'ad discontinuity, the margins are fragmented, and there are multiple short, subparallel axial segments (Fig. 10).

Figure 11 shows the mapped rift margins and axial segments. In this study, the term "mapped axial segments" is not simply correlated with rift axes, especially in the onshore regions. The geology in this region is quite complex, including several fault and transfer zones as well as exposed pre-rift rock sequences (e.g., Varet, 2018); however, the mapped axial segments are somewhat correlative with rift axes suggested based on field observations (e.g., Rime et al., 2023).

Within the Afar triangle, southwest to the Tendaho-Goba'ad discontinuity, the rift margins are continuous and smooth, and the axial volcanic range generally continues the trend of the axial valley of the Main Ethiopian Rift, reflecting a sub-perpendicular extension in accordance with the Nubia–Somalia kinematics and could thus be regarded as a rigid plate boundary.

Northeast of the Tendaho-Goba'ad discontinuity, axial segments are generally subparallel to the Red Sea axis (Zwaan et al., 2020b), which led to the interpretation of this region as an evolving discontinuity of the oceanic spreading center in the Red Sea (e.g., Tazieff et al., 1972; Bosworth et al., 2005). Although several focal solutions indicated dextral strike-slip motions in this area, we do not find other evidence for a typical first-order transform connection between the ridge in the Red Sea and the continuation of the northern Afar axial segments in the offshore Gulf of Zula. Magnetic isochrons in the Red Sea are mapped over 100 km south of the Gulf of Zula (Fig. 12), and the volcanic ridge in the southern Red Sea is very active (Eyles et al., 2018). Although earthquake clusters at 16.5° N indicate strike-slip solutions, supporting a structural connection to the Red Sea axis, these are abundant throughout the study area (Hofstetter and Beyth, 2003). Alternatively, the jump between the Red Sea ridge and the axial segments in northeastern Afar could be interpreted as a non-transform discontinuity; however, second-order discontinuities are usually characterized by < 30 km offsets, and here the jump is ∼ 200 km (Macdonald et al., 1984; Carbotte et al., 2016). Thus, there is no structural evidence to relate the axial volcanism in the Afar triangle to the Red Sea spreading center. This conclusion agrees with the study of Rime et al. (2023), which suggests a northward propagation of the rift in the Danakil depression mainly supported by younging of magmatic products and rifting ages.

The architecture of the intersection region northeast to the Tendaho-Goba'ad discontinuity reflects a rugged connection of the Red Sea and the Gulf of Aden arms to the Main Ethiopian Rift and is characterized by diffuse deformation rather than sharp plate boundaries. A recent model based on GPS observations (Viltres et al., 2020) reveals a
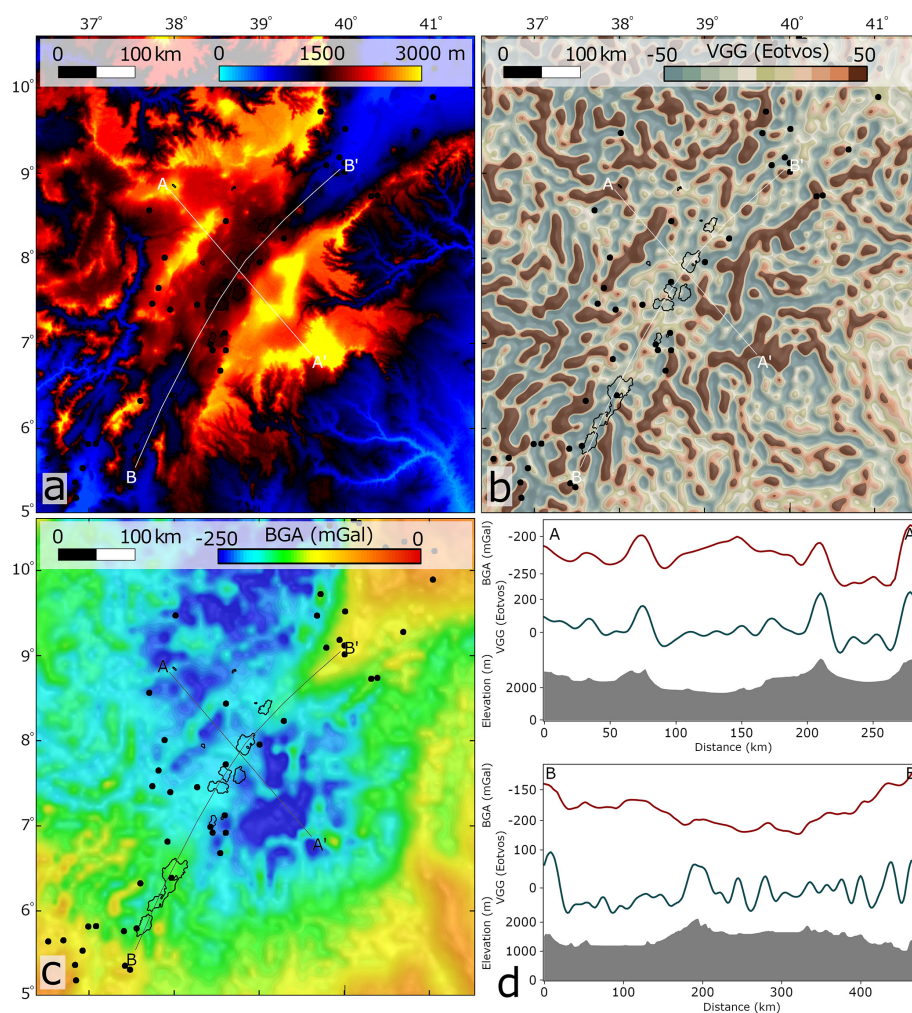
Figure 9. Topography **(a)**, vertical gravity gradient **(b)**, and Bouguer anomaly **(c)** in the northern Main Ethiopian Rift. Black dots indicate earthquake locations (ISC catalog). **(d)** Profiles across (AA') and along (BB') the rift valley.
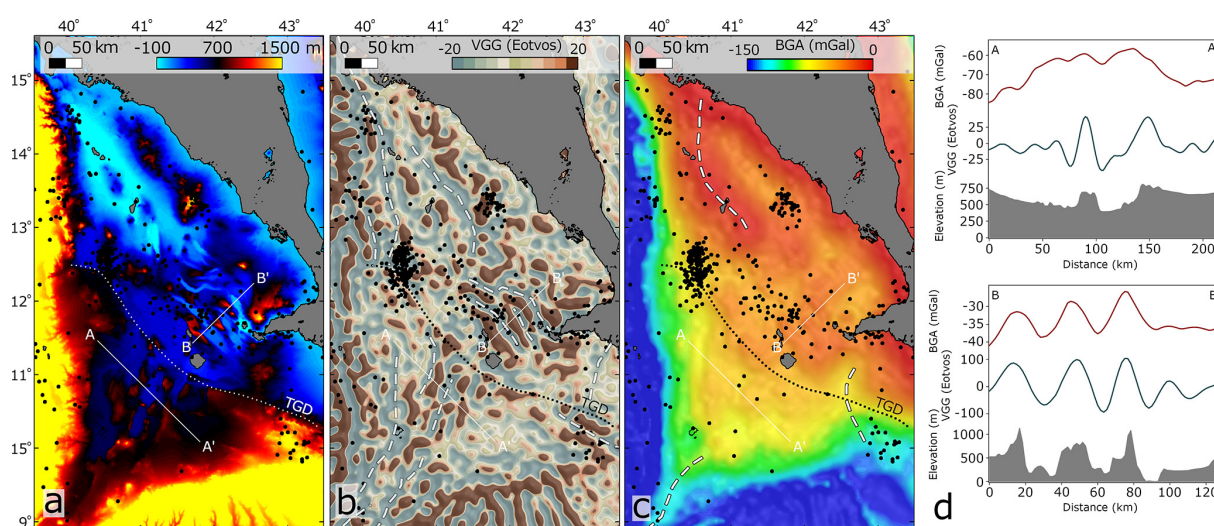

Figure 10. Topography **(a)**, vertical gravity gradient **(b)**, and Bouguer anomaly **(c)** in the Afar triangle. Black dots indicate earthquake locations (ISC catalog). TGD is the Tendaho-Goba'ad discontinuity. **(d)** Profiles SW (AA') and NE (BB') to the TGD.
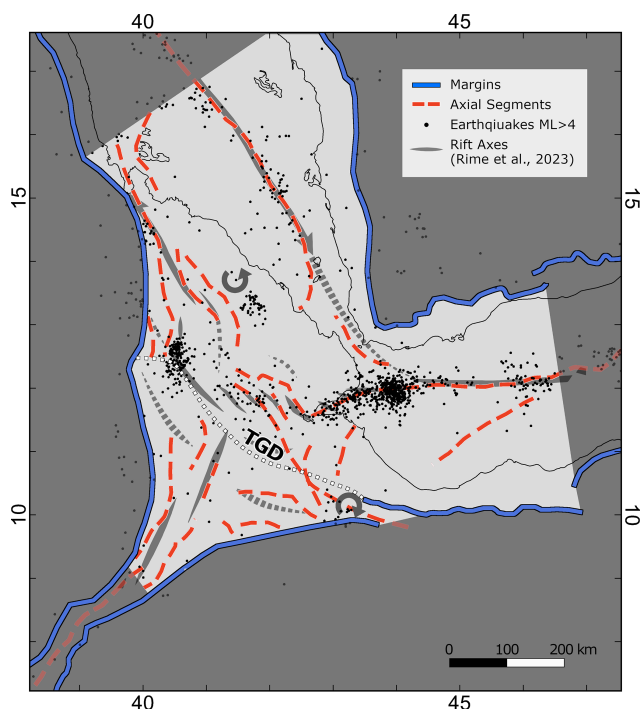
Figure 11. Rift margins (solid white lines) and axial segments (long dashed black lines) in the Afar region. Black dots indicate earthquake locations (ISC catalog). TGD is the Tendaho-Goba'ad discontinuity.
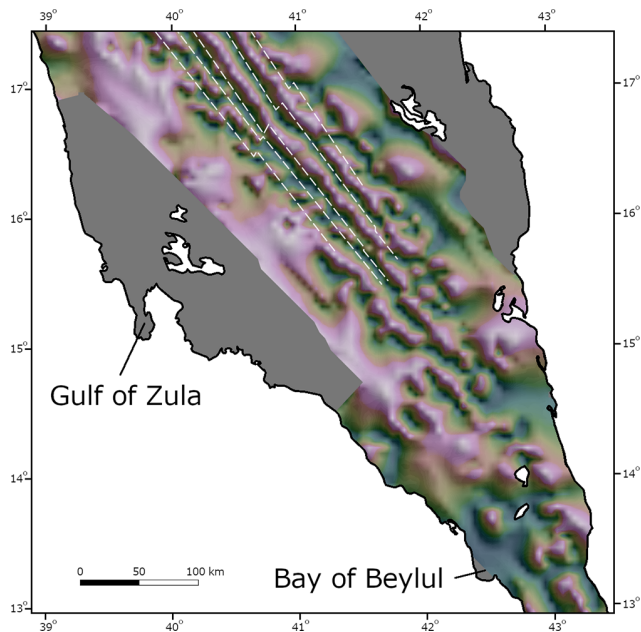

Figure 12. Tilt-angle derivative map of magnetic anomalies projected on a shaded relief after Issachar et al. (2022). Purple shades represent positive angles, and green shades represent negative angles. Dashed white lines indicate magnetic strips (Schettino et al., 2016).

diffuse Danakil–Nubia boundary with inter-rifting deformation over a zone > 100 km wide. The Danakil microplate extends to the Zukur–Hanish islands at its southern edge (∼ 13.8° N) with no precise or sharp boundary (Fig. 3). The Danakil microplate is rotating counterclockwise (at a mean rate of 1.5° ± 0.6° Ma for the last ∼ 7 Myr; Manighetti et al., 2001), while the Ali-Sabieh block, south of the Gulf of Tadjoura, is rotating clockwise (15° between 8 and 4 Ma; Audin et al., 2004), described as a "saloon-door" mode of opening (Fig. 11; Kidane, 2016).

The concept of segments of localized strain, which are spread over a broad zone in Afar, was noted from many indicators including diking events, structural geology, seismology, and geodesy (Keir et al., 2011; Pagli et al., 2014, 2018; Doubre et al., 2017). Analog models demonstrated that the plate interactions in Afar result in a broad zone of localized extension (Maestrelli et al., 2022).

Hence, the architecture of the intersection region of the rift arms encloses a ∼ 150 000 km^2 complex region, in which diffuse boundaries and microplate rotations link the three rift arms (Fig. 11). Accordingly, a genuinely single triple-junction point, in the sense of a three-rift-arm intersection point, cannot be specified for this system, and multiple triple junctions could be considered (e.g., see tectonic models in Viltres et al., 2020). The difficulty of defining sharp plate boundaries within Afar was discussed in many works (e.g., Barberi and Varet, 1977, and references therein). Nevertheless, we agree that the intersection point of the Ethiopian rift valley and the Tendaho-Goba'ad discontinuity could be regarded as the "main" junction point of the rift system, as the deformation characteristics between the northern Main Ethiopian Rift and the diffuse zone on the Gulf of Aden–Red Sea rifts are most distinctively changed there (Tesfaye et al., 2003).

7.2 Spatial constraints in the development of the plume–rift system

The mapping of the rift margins and axial segments allows us to draw two spatial constraints in the development of the plume–rift system.

1. The first is the connection of the Main Ethiopian Rift to the Gulf of Aden–Red Sea rifts by a northeastward propagation. Since the divergence between Nubia and Somalia is sub-perpendicular to the strike of the northern Main Ethiopian Rift, its propagation direction is not entirely dictated by the kinematics (Tesfaye et al., 2003; Wolfenden et al., 2004; Bonini et al., 2005; Keranen and Klemperer, 2008; Abebe et al., 2010). The margins of southeast Afar show symmetric, continuous, and smooth curved trends, from the elevated regions of the Main Ethiopian Rift to the Tendaho-Goba'ad discontinuity (Fig. 5). With respect to the northeastward trend of the Main Ethiopian Rift, the Somali margin is curved clockwise, following the Ali-Sabieh sense of rotation

(Kidane, 2016), whereas the Ethiopian margin is curved counterclockwise, like the Danakil sense of rotation (Fig. 11; Schult, 1974). This architecture could be understood in terms of fracture mechanics by the reorientation of a propagating fracture near a pre-existing fracture. Strain analysis indicates that a propagating fracture would curve parallel to the pre-existing fracture under a tensional stress field due to free surface boundary conditions induced by the open pre-existing fracture (Dyer, 1988). In analogy, the architecture of the study area express a smooth linkage of the Main Ethiopian Rift to the pre-existing Gulf of Aden–Red Sea rifts by a northeastward propagation. Hence, this implies that a triple junction formed at a late stage, when all three arms were already significantly developed. This conclusion agrees with structural geochronology within the northern Main Ethiopian Rift, showing that extension in the northern Main Ethiopian Rift commenced at 11 Ma (Wolfenden et al., 2004).

2. The second spatial constraint is the abandonment of an early tectonic connection between the Red Sea and the Gulf of Aden through the Bab al Mandab Strait. As the VGG and neovolcanic activity indicate that the Red Sea axis currently enters Afar at the Bay of Beylul (see Sect. 6.2), we find arguments for an earlier tectonic connection between the Red Sea and the Gulf of Aden through Bab al Mandab Strait: (i) south of 13.2° N and up to the connection to the Gulf of Aden (12.3° N), BGA and VGG depict the typical and previously defined gravity signature of the rift axis (Figs. 7 and 8; see Sect. 6.2). (ii) The submarine channel north to Hanish island (Fig. 7, 13.4° N) shows no association with modern water currents and possibly formed by faults in the subsurface (Mitchell and Sofianos, 2018). (iii) This is the straight continuation of the Red Sea axis, along which the basins are connected (Fig. 1). Thus, it is reasonable to propose that it was the tectonic connection during the early stages of rift development. Likewise, reconstructions suggest that the Danakil microplate started to rotate in the middle Miocene (∼ 10 Ma), when Arabia was already separated from Africa (Collet et al., 2000; Schettino et al., 2016; Rime et al., 2023). Those reconstructions show that the pre-middle Miocene divergence was focused along Danakil and Arabia at the southernmost Red Sea. This suggests that the present deflection of the rift axes at the tip of the Gulf of Aden and the Red Sea marks a tectonic reorganization in this region.

Adopting the fracture propagation analog postulated here for the northeastward propagation of the Main Ethiopian Rift implies that the new stress conditions in Afar may be responsible for the abandonment of the tectonic connection between the Red Sea and the Gulf of Aden. Rime et al. (2023) suggest that the deposition of lacustrine sediments (Chorora Fm)

recorded the development of the Main Ethiopian Rift in Afar. They point out that these sediments were deposited coeval with the individualization of the Danakil Block and thus with the decrease in the extensional tectonic activity at the southernmost Red Sea rift.

These two spatial constraints suggest that the onset of the triple junction occurred at a late stage when the three rift arms were already developed and the Red Sea was tectonically connected to the Gulf of Aden, ∼ 250 km away from the present-day triple junction (Fig. 13). The onset of the triple junction marked a tectonic reorganization and microplate formation. As a result, the Gulf of Aden and the Red Sea arms are not smoothly connected to the Main Ethiopian Rift, and a vast area of diffuse and complex deformation developed within the intersection region.

7.3 Mechanisms for plume–rift association

The temporal constraints regarding the development of the plume–rift features, summarized in Sect. 4, together with the two spatial constraints inferred in this study, allow us to examine the causal relationship between the activity of the Afar plume and rifting. Our insights suggest that neither active nor passive rifting mechanisms are solely consistent with observations. Passive rifting models fail to explain the plume–rift association, mainly because flood basalt volcanism cannot be attributed to a passively rising asthenospheric mantle beneath a stretched and thinned lithosphere, as dynamic uplift in Ethiopia is a long-lasting process that preceded flood basalt volcanism (Sembroni et al., 2016). Hence, rifting and associated subsidence are subsequent to flood basalt volcanism (Fig. 4). The estimations that the Ethiopian plateau was elevated ∼ 1 km before flood basalts (Fig. 4) coincide with active plume-head predictions (Campbell and Griffiths, 1990). Moreover, the passive model does not explain why a triple junction is located within the flood basalt area, as rifting in the Red Sea and Gulf of Aden is at an oblique angle to the former sutures (Buiter and Torsvik, 2014).

On the other hand, active models are not in line with the progressive development of the rifts, mainly because the flood basalt region cannot be considered a center or a nucleus from which rift arms spread, as expected in an actively generated triple junction. Numerous studies noted that the tectonic development of the Afar region is not compatible with a simplified model of rift arms that simultaneously spread away from a triple junction (see Sect. 5.2 in Rime et al., 2023, for a review). The triple junction was the last feature to develop in the system through the propagation of the Main Ethiopian Rift towards Afar, followed by a tectonic reorganization including the abandonment of a former tectonic connection between the Red Sea and the Gulf of Aden. By this time, the rift arms had already developed, and the break-up between Africa and Arabia had already been accomplished. This tectonic reorganization cannot be attributed to the development of gravitational forces exerted by the plume head
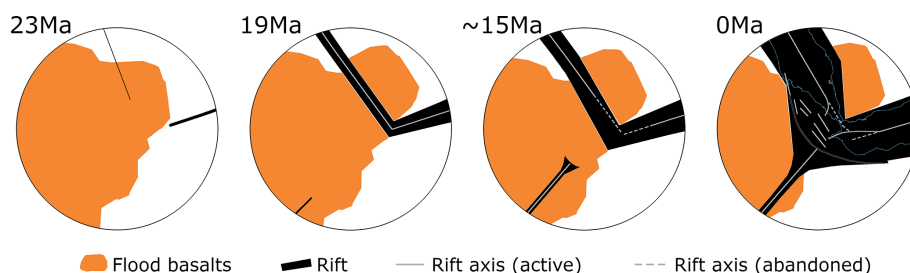
Figure 13. Synthesis of the progressive development of the rift intersections.

(Hill, 1991), as it occurred ∼ 20 Myr after flood basalt magmatism. That rules out the possibility that the arrival of the Afar plume directly led to the formation of the triple junction and the rift arms did not spread from the plume region.

We propose a scenario in which rifting was triggered by a plume-induced plate rotation (Fig. 2c). Numerical simulations suggest that horizontal asthenospheric flows due to the arrival of a plume head at the base of the lithosphere induce a plume push force that can accelerate plates by several centimeters per year (van Hinsbergen et al., 2011, 2021; Pusok and Stegman, 2020). In this scenario, flood basalt volcanism would be synchronous with an abrupt plate speed-up and thus with new remote stress conditions. In the case of the Indian plate, at least two episodes of massive flood basalt volcanism, the Morondava LIP (∼ 94 Ma) and Deccan traps (67 Ma), are associated with plume-derived plate acceleration and a drastic change in the tectonic framework (van Hinsbergen et al., 2011, 2021; Cande and Stegman, 2011; Pusok and Stegman, 2020). Further, torque balance modeling simulating the horizontal forces generated from a point source (plume head) suggests that horizontal plume push can force a significant plate rotation and, consequently, initiate new plate boundaries (van Hinsbergen et al., 2021).

In the Afro-Arabian rift, new plate boundaries indeed formed after the arrival of the large Afar plume, and a significant plate rotation of Arabia around a nearby pole characterizes the Arabian continent (Joffe and Garfunkel, 1987; Viltres et al., 2022). Magnetic anomalies and structural reconstructions suggest that the rotation around a nearby pole already characterized Arabia since the Oligocene (Fournier et al., 2010; Schettino et al., 2018). Additionally, the beginning of intensive volcanism in the northwestern Arabian plate (Harrat Ash Shaam) in the late Oligocene (Ilani et al., 2001) reflected a change in mantle–crust interaction and intracontinental extension within the Arabian plate, adjacent to the arrival of Afar plume (Garfunkel, 1989). In the Harrat Ash Shaam volcanic field, diking directions from Miocene to recent ages record the rotation of Arabia (Giannerini et al., 1988), suggesting that during the first stages of volcanism the Arabian plate was already rotating around a nearby pole.

The arrival of the Afar plume was also accompanied by a slowdown of Africa (Le Pichon and Gaulier, 1988). By this time, Africa collided with Eurasia in the west, explaining its slowdown (Jolivet and Faccenna, 2000) and increased intraplate volcanism (Burke, 1996). However, this collision of Africa and Eurasia cannot simply resolve the change in the rotation of Arabia as the Arabian continent collided with Eurasia not earlier than ∼ 18 Ma (Su and Zhou, 2020), although some authors have suggested that asymmetrical along-trench entrance of continental material could lead to an intraplate extension similar to those that generated the Africa–Arabia break-up (Bellahsen et al., 2003). Faccenna et al. (2013) show that plume push from the Afar area resolves the present-day plate kinematics in the Middle East, particularly the anticlockwise toroidal pattern of the Arabia–Anatolia–Aegean system. The importance of active upwelling in Afar to lateral mantle flow below Arabia is also illustrated by shear-wave splitting, indicating a general N–S anisotropy in the mantle (Qaysi et al., 2018). Stamps et al. (2014) calculated the current driving forces for the Nubia–Somalia divergence and found that gravitational potential energy is the most significant force, stronger by an order of magnitude than forces from basal shear tractions of mantle convection. They point out that the gravitational potential energy is sufficient to sustain present-day rifting in East Africa but not to initiate rupture of continental lithosphere. In the case of the Arabian plate, basal shear tractions are expected to be higher due to the orientation of northward-directed mantle flow (Faccenna et al., 2013).

Plume-induced plate rotation settles the fact that regional uplift and flood basalt volcanism shortly preceded rifting (Sembroni et al., 2016), together with the insight that rifting was developed by far-field forces and plate kinematics (Autin et al., 2013; Bosworth and Stockli, 2016). It also explains why the rifts intersect within the plume region as the lithosphere in this region was weakened by the hot plume material (François et al., 2018). Finally, it explains the delayed development of the Main Ethiopian Rift and the late onset of the Afar triple junction by its northwestward propagation, as these were controlled by the slower kinematics of the Somali plate rather than dynamic forces. In this tectonic scenario, active and passive mechanisms are coupled and have positive feedback, allowing a close occurrence of flood basalt volcanism and continental break-up, alongside passive rifting.

8   Summary and conclusions

We reviewed the geologic setting of the Afro-Arabian rift, in which vast regions of flood basalts and ongoing continental break-up are superimposed, aiming to infer a causal relationship between the activity of the deep-seated Afar plume and crustal break-up. We explored the R-R-R triple junction between the Gulf of Aden, the Red Sea, and the Main Ethiopian Rift that divides the large Cenozoic plume-related flood basalt series in Ethiopia and Yemen. Based on the interpretation of topography, bathymetry and gravity, as well as the integration of magnetic anomalies, earthquakes, and volcano distribution, we mapped the margins and axes of the rift arms.

Our results show that the terminations of the Gulf of Aden and the Red Sea arms are rough and irregular, in contrast to the symmetric, continuous, and smooth architecture of the Main Ethiopian Rift. The triple junction formed through the northeastward propagation of the Main Ethiopian Rift and the abandonment of the tectonic connection between the Red Sea and the Gulf of Aden through Bab al Mandab Strait. This suggests a progressive development of a broad region of diffuse deformation at the intersection area. The triple junction was the last feature to develop in the plume–rift system after all rift arms were sufficiently evolved and the break-up between Africa and Arabia was already accomplished.

This progressive development does not align with the classic active rifting model, which predicts a plume-generated triple junction at the locus of the rift development. Nevertheless, the classic passive rifting model fails to explain the chronological evidence, as flood basalts probably erupted on elevated topography before rifting started. We discuss a scenario of plume-induced plate rotation in which the arrival of the Afar plume triggered the rotation of Arabia around a nearby pole that has characterized the system since the Oligocene. We argue that plume-induced plate rotation better explains the progressive development of the plume–rift system in the Afro-Arabian rift.

Data availability. The bathymetry and topography data used in this study were retrieved from the GEBCO Compilation Group (2021) and are available at https://doi.org/10.5285/c6612cbe-50b3-0cff-e053-6c86abc09f8f.

The VGG data used in this study are available at https://topex.ucsd.edu/grav_outreach/ (Sandwell et al., 2014).

The BGA data used in this study are available at https://doi.org/10.5880/ICGEM.2019.007 (model XGM2019e-2159, "gravity_anomaly_bg"; Zingerle et al., 2019).

Earthquake data were retrieved from the International Seismological Centre (2020) online bulletin at https://doi.org/10.31905/D808B830.

Quaternary onshore volcano locations were retrieved from the Global Volcanism Program, Smithsonian Institution, available at https://doi.org/10.5479/si.GVP.VOTW5-2024.5.2 (Global Volcanism Program, 2024).

Magnetic anomalies data are available at https://figshare.com/articles/dataset/Transcurrent_Regimes_During_Rotational_Rifting_New_Insights_from_Magnetic_Anomalies_in_the_Red_Sea/14743272 (Issachar et al., 2022).

References

Abebe, T., Balestrieri, M. L., and Bigazzi, G.: The Central Main Ethiopian Rift is younger than 8 Ma: confirmation through apatite fission-track thermochronology, Terra Nova, 22, 470–476, https://doi.org/10.1111/j.1365-3121.2010.00968.x, 2010.

Akram, F., Garcia, M. A., and Puig, D.: Active contours driven by difference of Gaussians, Sci. Rep., 7, 1–15, https://doi.org/10.1038/s41598-017-14502-w, 2017.

Anderson, D. L.: The sublithospheric mantle as the source of continental flood basalts; the case against the continental lithosphere and plume head reservoirs, Earth Planet. Sc. Lett., 123, 269–280, https://doi.org/10.1016/0012-821X(94)90273-9, 1994.

Anderson, D. L.: Large Igneous Provinces, Delamination, and Fertile Mantle, Elements, 1, 271–275, https://doi.org/10.2113/gselements.1.5.271, 2005.

Augustin, N., van der Zwan, F. M., Devey, C. W., and Brandsdóttir, B.: 13 million years of seafloor spreading throughout the Red Sea Basin, Nat. Commun., 12, 1–10, https://doi.org/10.1038/s41467-021-22586-2, 2021.

Audin, L., Quidelleur, X., Coulié, E., Courtillot, V., Gilder, S., Manighetti, I., Gillot, P.-Y., Tapponnier, P., and Kidane, T.: Palaeomagnetism and K--Ar and ^{40}Ar/^{39}Ar ages in the Ali Sabieh area (Republic of Djibouti and Ethiopia): constraints on the mechanism of Aden ridge propagation into southeastern Afar during the last 10 Myr, Geophys. J. Int., 158, 327–345, https://doi.org/10.1111/j.1365-246X.2004.02286.x, 2004.

Autin, J., Bellahsen, N., Leroy, S., Husson, L., Beslier, M. O., and d'Acremont, E.: The role of structural inheritance in oblique rifting: Insights from analogue models and application to the Gulf of Aden, Tectonophysics, 607, 51–64, https://doi.org/10.1016/j.tecto.2013.05.041, 2013.

Barberi, F. and Varet, J.: Volcanism of Afar: Small-scale plate tectonics implications, GSA Bull., 88, 1251–1266, https://doi.org/10.1130/0016-7606(1977)88<1251:VOASPT>2.0.CO;2, 1977.

Bellahsen, N., Faccenna, C., Funiciello, F., Daniel, J. M., and Jolivet, L.: Why did Arabia separate from Africa? Insights from 3-D laboratory experiments, Earth Planet. Sc. Lett., 216, 365–381, https://doi.org/10.1016/S0012-821X(03)00516-8, 2003.

Bellahsen, N., Husson, L., Autin, J., Leroy, S., and D'Acremont, E.: The effect of thermal weakening and buoyancy forces on rift localization: Field evidences from the Gulf of Aden oblique rifting, Tectonophysics, 607, 80–97, https://doi.org/10.1016/j.tecto.2013.05.042, 2013.

Bellieni, G., Visentin, E.J., Zanettin, B., Piccirillo, E. M., Radicati di Brozolo, F., and Rita, F.: Oligocene transitional tholeiitic magmatism in Northern turkana (Kenya): Comparison with the Coeval Ethiopian volcanism, Bull. Volcanol., 44, 411–427, https://doi.org/10.1007/BF02600573, 1981.

Beyene, A. and Abdelsalam, M. G.: Tectonics of the Afar Depression: A review and synthesis, J. Afr. Earth Sci., 41, 41–59, https://doi.org/10.1016/j.jafrearsci.2005.03.003, 2005.

Bonini, M., Corti, G., Innocenti, F., Manetti, P., Mazzarini, F., Abebe, T., and Pecskay, Z.: Evolution of the Main Ethiopian Rift in the frame of Afar and Kenya rifts propagation, Tectonics, 24, TC1007, https://doi.org/10.1029/2004TC001680, 2005.

Bosworth, W.: Geological evolution of the Red Sea: historical background, review, and synthesis, in: In The Red Sea, Springer, Berlin, Heidelberg, 45–78, https://doi.org/10.1007/978-3-662-45201-1, 2015.

Bosworth, W. and Stockli, D. F.: Early magmatism in the greater Red Sea rift: Timing and significance, Can. J. Earth Sci., 53, 1158–1176, https://doi.org/10.1139/cjes-2016-0019, 2016.

Bosworth, W., Huchon, P., and McClay, K.: The Red Sea and Gulf of Aden Basins, J. Afr. Earth Sci., 43, 334–378, https://doi.org/10.1016/j.jafrearsci.2005.07.020, 2005.

Bridges, D. L., Mickus, K., Gao, S. S., Abdelsalam, M. G., and Alemu, A.: Magnetic stripes of a transitional continental rift in Afar, Geology, 40, 203–206, https://doi.org/10.1130/G32697.1, 2012.

Bryan, S. E. and Ferrari, L.: Large igneous provinces and silicic large igneous provinces: Progress in our understanding over the last 25 years, GSA Bull., 125, 1053–1078, https://doi.org/10.1130/B30820.1, 2013.

Buiter, S. J. H. and Torsvik, T. H.: A review of Wilson Cycle plate margins: A role for mantle plumes in continental break-up along sutures?, Gondwana Res., 26, 627–653, https://doi.org/10.1016/J.GR.2014.02.007, 2014.

Burke, K.: The African Plate, S. Afr. J. Geol., 99, 341–409, https://hdl.handle.net/10520/EJC-942801f20 (last access: 26 June 2024), 1996.

Burke, K. and Dewey, J. F.: Plume-generated triple junctions: key indicators in applying plate tectonics to old rocks, J. Geol., 81, 406–433, https://doi.org/10.1086/627882, 1973.

Campbell, I. H. and Griffiths, R. W.: Implications of mantle plume structure for the evolution of flood basalts, Earth Planet. Sc. Lett., 99, 79–93, https://doi.org/10.1016/0012-821X(90)90072-6, 1990.

Cande, S. C. and Stegman, D. R.: Indian and African plate motions driven by the push force of the Réunion plume head, Nature, 475, 47–52, https://doi.org/10.1038/nature10174, 2011.

Carbotte, S. M., Smith, D. K., Cannat, M., and Klein, E. M.: Tectonic and magmatic segmentation of the Global Ocean Ridge System: A synthesis of observations, Geol. Soc. Spec. Publ., 420, 249–295, https://doi.org/10.1144/SP420.5, 2016.

Chatterjee, S., Goswami, A., and Scotese, C. R.: The longest voyage: Tectonic, magmatic, and paleoclimatic evolution of the Indian plate during its northward flight from Gondwana to Asia, Gondwana Res., 23, 238–267, https://doi.org/10.1016/j.gr.2012.07.001, 2013.

Chorowicz, J.: The East African rift system, J. Afr. Earth Sci., 43, 379–410, https://doi.org/10.1016/j.jafrearsci.2005.07.019, 2005.

Collet, B., Taud, H., Parrot, J. F., Bonavia, F., and Chorowicz, J.: A new kinematic approach for the Danakil block using a Digital Elevation Model representation, Tectonophysics, 316, 343–357, https://doi.org/10.1016/S0040-1951(99)00263-2, 2000.

Corti, G.: Continental rift evolution: From rift initiation to incipient break-up in the Main Ethiopian Rift, East Africa, Earth-Sci. Rev., 96, 1–53, https://doi.org/10.1016/j.earscirev.2009.06.005, 2009.

Coulié, E., Quidelleur, X., Courtillot, V., Lefèvre, J. C., and Chiesa, S.: Comparative K-Ar and Ar/Ar dating of Ethiopian and Yemenite Oligocene volcanism: Implications for timing and duration of the Ethiopian traps, Earth Planet. Sc. Lett., 206, 477–492, https://doi.org/10.1016/S0012-821X(02)01089-0, 2003.

Courtillot, V., Jaupart, C., Manighetti, I., Tapponnier, P., and Besse, J.: On causal links between flood basalts and continental breakup, Earth Planet. Sc. Lett., 166, 177–195, https://doi.org/10.1016/S0012-821X(98)00282-9, 1999.

DeMets, C. and Merkouriev, S.: High-resolution estimates of Nubia-Somalia plate motion since 20 Ma from reconstructions of the Southwest Indian Ridge, Red Sea and Gulf of Aden, Geophys. J. Int., 207, 317–332, https://doi.org/10.1093/gji/ggw276, 2016.

Doubre, C., Deprez, A., Masson, F., Socquet, A., Lewi, E., Grandin, R., Nercessian, A., Ulrich, P., De Chabalier, J. B., Saad, I. and Abayazid, A.: Current deformation in Central Afar and triple junction kinematics deduced from GPS and InSAR measurements, Geophys. J. Int., 208, 936–953, https://doi.org/10.1093/gji/ggw434, 2017.

Duclaux, G., Huismans, R. S., and May, D. A.: Rotation, narrowing, and preferential reactivation of brittle structures during oblique rifting, Earth Planet. Sc. Lett., 531, 115952, https://doi.org/10.1016/j.epsl.2019.115952, 2020.

Dyer, R.: Using joint interactions to estimate paleostress ratios, J. Struct. Geol., 10, 685–699, https://doi.org/10.1016/0191-8141(88)90076-4, 1988.

Ebinger, C. J., Keir, D., Bastow, I. D., Whaler, K., Hammond, J. O. S., Ayele, A., Miller, M. S., Tiberi, C., and Hautot, S.: Crustal Structure of Active Deformation Zones in Africa: Implications for Global Crustal Processes, Tectonics, 36, 3298–3332, https://doi.org/10.1002/2017TC004526, 2017.

Ernst, R. E.: Large igneous provinces, Cambridge Univ. Press, ISBN 0521871778, 2014.

Eyles, J. H. W., Illsley-Kemp, F., Keir, D., Ruch, J., and Jónsson, S.: Seismicity Associated With the Formation of a New Island in the Southern Red Sea, Front. Earth Sci., 6, 1–10, https://doi.org/10.3389/feart.2018.00141, 2018.

Faccenna, C., Becker, T. W., Jolivet, L., and Keskin, M.: Mantle convection in the Middle East: Reconciling Afar upwelling, Arabia indentation and Aegean trench rollback, Earth Planet. Sc. Lett., 375, 254–269, https://doi.org/10.1016/J.EPSL.2013.05.043, 2013.

Faccenna, C., Glišović, P., Forte, A., Becker, T. W., Garzanti, E., Sembroni, A., and Gvirtzman, Z.: Role of dynamic topography in sustaining the Nile River over 30 million years, Nat. Geosci., 12, 1012–1017, https://doi.org/10.1038/s41561-019-0472-x, 2019.

Forsyth, D. and Uyeda, S.: On the relative importance of the driving forces of plate motion, Geophys. J. Int., 43, 163–200, 1975.

Fournier, M., Chamot-Rooke, N., Petit, C., Huchon, P., Al-Kathiri, A., Audin, L., Beslier, M. O., d'Acremont, E., Fabbri, O., Fleury, J. M., and Khanbari, K.: Arabia-Somalia plate kinematics, evolution of the Aden-OwenCarlsberg triple junction, and opening of the Gulf of Aden, J. Geophys. Res.-Solid, 115, 1–24, https://doi.org/10.1029/2008JB006257, 2010.

François, T., Koptev, A., Cloetingh, S., Burov, E., and Gerya, T.: Plume-lithosphere interactions in rifted margin tectonic settings: Inferences from thermo-mechanical modelling, Tectonophysics, 746, 138–154, https://doi.org/10.1016/j.tecto.2017.11.027, 2018.

Frizon De Lamotte, D., Fourdan, B., Leleu, S., Leparmentier, F., and De Clarens, P.: Style of rifting and the stages of Pangea breakup, Tectonics, 34, 1009–1029, https://doi.org/10.1002/2014TC003760, 2015.

Fromm, T., Planert, L., Jokat, W., Ryberg, T., Behrmann, J. H., Weber, M. H., and Haberland, C.: South Atlantic opening: A plume-induced breakup?, Geology, 43, 931–934, https://doi.org/10.1130/G36936.1, 2015.

Garfunkel, Z.: Tectonic setting of phanerozoic magmatism in Israel, Isr. J. Earth Sci., 38, 51–74, 1989.

Garfunkel, Z. and Beyth, M.: Constraints on the structural development of Afar imposed by the kinematics of the major surrounding plates, Geol. Soc. Spec. Publ., 259, 23–42, https://doi.org/10.1144/GSL.SP.2006.259.01.04, 2006.

Gass, I. G., Mallick, D. I. J., and Cos, K. G.: Volcanic islands of the Red Sea, J. Geol. Soc., 129, 275–309, https://doi.org/10.1144/gsjgs.129.3.0275, 1973.

GEBCO Compilation Group: The GEBCO_2019 Grid: a continuous terrain model of the global oceans and land, GEBCO Compilation Group GEBCO 2021 Grid [data

set], https://doi.org/10.5285/c6612cbe-50b3-0cff-e053-6c86abc09f8f, 2021.

Geoffroy, L.: Volcanic passive margins, C. R. Geosci., 337, 1395–1408, https://doi.org/10.1016/J.CRTE.2005.10.006, 2005.

George, R., Rogers, N., and Kelley, S.: Earliest magmatism in Ethiopia: Evidence for two mantle plumes in one flood basalt province, Geology, 26, 923–926, https://doi.org/10.1130/0091-7613(1998)026<0923:EMIEEF>2.3.CO;2, 1998.

Giannerini, G., Campredon, R., Feraud, G., and Abou Zakhem, B.: Deformations intraplaques et volcanisme associe; exemple de la bordure NW de la plaque Arabique au Cenozoique, Bull. Soc. Geol. Fr., IV, 937–947, https://doi.org/10.2113/gssgfbull.IV.6.937, 1988.

Gillard, M., Leroy, S., Cannat, M., and Sloan, H.: Margin-to-Margin Seafloor Spreading in the Eastern Gulf of Aden: A 16 Ma-Long History of Deformation and Magmatism from Seismic Reflection, Gravity and Magnetic Data, Front. Earth Sci., 9, 628, https://doi.org/10.3389/feart.2021.707721, 2021.

Girdler, R. W., and Styles, P.: Two stage Red Sea floor spreading, Nature, 247, 7–11, https://doi.org/10.1038/247007a0, 1974.

Global Volcanism Program: Volcanoes of the World, v. 5.2.0, Smithsonian Institution [data set], https://doi.org/10.5479/si.GVP.VOTW5-2024.5.2, 2024.

Gvirtzman, Z., Faccenna, C., and Becker, T. W.: Isostasy, flexure, and dynamic topography, Tectonophysics, 683, 255–271, https://doi.org/10.1016/j.tecto.2016.05.041, 2016.

Hill, R. I.: Starting plumes and continental break-up, Earth Planet. Sc. Lett., 104, 398–416, https://doi.org/10.1016/0012-821X(91)90218-7, 1991.

Hofstetter, R. and Beyth, M.: The afar depression: Interpretation of the 1960–2000 earthquakes, Geophys. J. Int., 155, 715–732, https://doi.org/10.1046/j.1365-246X.2003.02080.x, 2003.

Hughes, G. W., Varol, O., and Beydoun, Z. R.: Evidence for Middle Oligocene rifting of the Gulf of Aden and for Late Oligocene rifting of the southern Red Sea, Mar. Petrol. Geol., 8, 354–358, https://doi.org/10.1016/0264-8172(91)90088-I, 1991.

Huismans, R. S., Podladchikov, Y. Y., and Cloetingh, S.: Transition from passive to active rifting: Relative importance of asthenospheric doming and passive extension of the lithosphere, J. Geophys. Res.-Solid, 106, 11271–11291, https://doi.org/10.1029/2000JB900424, 2001.

Ilani, S., Harlavan, Y., Tarawneh, K., Rabba, I., Weinberger, R., Ibrahim, K., Peltz, S., and Steinitz, G.: New K-Ar ages of basalts from the Harrat Ash Shaam volcanic field in Jordan: Implications for the span and duration of the upper-mantle upwelling beneath the western Arabian plate, Geology, 29, 171–174, https://doi.org/10.1130/0091-7613(2001)029<0171:NKAAOB>2.0.CO;2, 2001.

Ince, E. S., Barthelmes, F., Reißland, S., Elger, K., Förste, C., Flechtner, F., and Schuh, H.: ICGEM – 15 years of successful collection and distribution of global gravitational models, associated services, and future plans, Earth Syst. Sci. Data, 11, 647–674, https://doi.org/10.5194/essd-11-647-2019, 2019.

International Seismological Centre: On-line Bulletin, International Seismological Centre [data set], https://doi.org/10.31905/D808B830, 2020.

Issachar, R., Ebbing, J., and Dilixiati, Y.: New magnetic anomaly map for the Red Sea reveals transtensional structures associated with rotational rifting, Sci. Rep., 12, 1–13,

https://doi.org/10.1038/s41598-022-09770-0, 2022 (data available at: https://figshare.com/articles/dataset/Transcurrent_Regimes_During_Rotational_Rifting_New_Insights_from_Magnetic_Anomalies_in_the_Red_Sea/14743272, last access: 9 July 2024).

Ivanov, A. V., Demonterova, E. I., He, H., Perepelov, A. B., Travin, A. V., and Lebedev, V. A.: Volcanism in the Baikal rift: 40 years of active-versus-passive model discussion, Earth-Sci. Rev., 148, 18–43, https://doi.org/10.1016/j.earscirev.2015.05.011, 2015.

Joffe, S. and Garfunkel, Z.: Plate kinematics of the Red Sea – a re-evaluation, Tectonophysics, 141, 5–22, 1987.

Jolivet, L. and Faccenna, C.: Mediterranean extension and the Africa-Eurasia collision, Tectonics, 19, 1095–1106, https://doi.org/10.1029/2000TC900018, 2000.

Keen, C. E.: The dynamics of rifting: deformation of the lithosphere by active and passive driving forces, Geophys. J. R. Astr. Soc., 80, 95–120, 1985.

Keir, D., Pagli, C., Bastow, I. D., and Ayele, A.: The magma-assisted removal of Arabia in Afar: Evidence from dike injection in the Ethiopian rift captured using InSAR and seismicity, Tectonics, 30, TC2008, https://doi.org/10.1029/2010TC002785, 2011.

Keir, D., Bastow, I. D., Pagli, C., and Chambers, E. L.: The development of extension and magmatism in the Red Sea rift of Afar, Tectonophysics, 607, 98–114, https://doi.org/10.1016/j.tecto.2012.10.015, 2013.

Keranen, K. and Klemperer, S. L.: Discontinuous and diachronous evolution of the Main Ethiopian Rift: Implications for development of continental rifts, Earth Planet. Sc. Lett., 265, 96–111, https://doi.org/10.1016/j.epsl.2007.09.038, 2008.

Kidane, T.: Strong clockwise block rotation of the Ali-Sabieh/Aïsha Block: Evidence for opening of the Afar Depression by a "saloon-door" mechanism, Geol. Soc. Spec. Publ., 420, 209–219, https://doi.org/10.1144/SP420.10, 2016.

Koppers, A. A., Becker, T. W., Jackson, M. G., Konrad, K., Müller, R. D., Romanowicz, B., Steinberger, B., and Whittaker, J. M.: Mantle plumes and their role in Earth processes, Nat. Rev. Earth Environ., 2, 382–401, https://doi.org/10.1038/s43017-021-00168-6, 2021.

Koptev, A., Gerya, T., Calais, E., Leroy, S., and Burov, E.: Afar triple junction triggered by plume-assisted bi-directional continental break-up, Sci. Rep., 8, 1–7, https://doi.org/10.1038/s41598-018-33117-3, 2018.

Le Pichon, X. and Gaulier, J.-M.: The rotation of Arabia and the Levant fault system, Tectonophysics, 153, 271–294, https://doi.org/10.1016/0040-1951(88)90020-0, 1988.

Leroy, S., Razin, P., Autin, J., Bache, F., d'Acremont, E., Watremez, L., Robinet, J., Baurion, C., Denèle, Y., Bellahsen, N., and Lucazeau, F.: From rifting to oceanic spreading in the Gulf of Aden: A synthesis, Front. Earth Sci., 5, 385–427, https://doi.org/10.1007/978-3-642-30609-9_20, 2013.

Lithgow-Bertelloni, C. and Silver, P. G.: Dynamic topography, plate driving forces and the African superswell, Nature, 395, 269–272, https://doi.org/10.1038/26212, 1998.

Macdonald, K., Sempere, J. C., and Fox, P. J.: East Pacific Rise from Siqueiros to Orozco fracture zones: along-strike continuity of axial neovolcanic zone and structure and evolution of overlapping spreading centers, J. Geophys. Res., 89, 6049–6069, https://doi.org/10.1029/JB089iB07p06049, 1984.

Maestrelli, D., Brune, S., Corti, G., Keir, D., Muluneh, A. A., and Sani, F.: Analog and Numerical Modeling of Rift-Rift-Rift Triple Junctions, Tectonics, 41, e2022TC007491, https://doi.org/10.1029/2022TC007491, 2022.

Manighetti, I., Tapponnier, P., Courtillot, V., Gallet, Y., Jacques, E., and Gillot, P. Y.: Strain transfer between disconnected, propagating rifts in Afar, J. Geophys. Res.-Solid, 106, 13613–13665, https://doi.org/10.1029/2000jb900454, 2001.

Mattash, M. A., Pinarelli, L., Vaselli, O., Minissale, A., Al-Kadasi, M., Shawki, M. N., and Tassi, F.: Continental Flood Basalts and Rifting: Geochemistry of Cenozoic Yemen Volcanic Province, Int. J. Geosci., 4, 1459–1466, https://doi.org/10.4236/ijg.2013.410143, 2013.

McConnell, R. and Baker, B.: The Structural Pattern of the Afro-Arabian Rift System in Relation to Plate Tectonics: Discussion, Philos. T. Roy. Soc. Lond. A, 267, 390–391, 1970.

McDougall, I. and Brown, F. H.: Timing of volcanism and evolution of the northern Kenya Rift, Geol. Mag., 146, 34–47, https://doi.org/10.1017/S0016756808005347, 2009.

Meshesha, D. and Shinjo, R.: Rethinking geochemical feature of the Afar and Kenya mantle plumes and geodynamics implications, J. Geophys. Res.-Solid, 113, 9209, https://doi.org/10.1029/2007JB005549, 2008.

Mitchell, N. C. and Sofianos, S. S.: Origin of submarine channel north of hanish sill, red sea, in: Geological Setting, Palaeoenvironment and Archaeology of the Red Sea, Springer International Publishing, 259–273, https://doi.org/10.1007/978-3-319-99408-6_12, 2018.

Mitchell, N. C., and Bosworth, W.: The tectonic stability of Arabia, In Rifting and sediments in the Red Sea and Arabian Gulf regions, CRC Press, 75–94, https://doi.org/10.1201/9781003321415-6, 2023.

Mitra, S., Mitra, K., Gupta, S., Bhattacharya, S., Chauhan, P., and Jain, N.: Alteration and submergence of basalts in Kachchh, Gujarat, India: implications for the role of the Deccan Traps in the India–Seychelles break-up, Geol. Soc. Lond. Spec. Publ., 445, 47–67, https://doi.org/10.1144/SP445.9, 2017.

Morag, N., Haviv, I., Eyal, M., Kohn, B. P., and Feinstein, S.: Early flank uplift along the Suez Rift: Implications for the role of mantle plumes and the onset of the Dead Sea Transform, Earth Planet. Sc. Lett., 516, 56–65, https://doi.org/10.1016/j.epsl.2019.03.002, 2019.

Moretti, I. and Froidevaux, C.: Thermomechanical models of active rifting, Tectonics, 5, 501–511, https://doi.org/10.1029/TC005I004P00501, 1986.

Morgan, W. J.: Convection plumes in the lower mantle, Nature, 230, 42–43, https://doi.org/10.1038/230042a0, 1971.

Okwokwo, O. I., Mitchell, N. C., Shi, W., Stewart, I. C. F., and Izzeldin, A. Y.: How have thick evaporites affected early seafloor spreading magnetic anomalies in the Central Red Sea?, Geophys. J. Int., 229, 1550–1566, https://doi.org/10.1093/gji/ggac012, 2022.

Pagli, C., Wang, H., Wright, T. J., Calais, E., and Lewi, E.: Current plate boundary deformation of the Afar rift from a 3-D velocity field inversion of InSAR and GPS, J. Geophys. Res.-Solid, 119, 8562–8575, https://doi.org/10.1002/2014JB011391, 2014.

Pagli, C., Yun, S.-H., Ebinger, C., Keir, D., and Wang, H.: Strike-slip tectonics during rift linkage, Geology, 47, 31–34, https://doi.org/10.1130/G45345.1, 2018.

Peate, I. U., Baker, J. A., Al-Kadasi, M., Al-Subbary, A., Knight, K. B., Riisager, P., Thirlwall, M. F., Peate, D. W., Renne, P. R., and Menzies, M. A.: Volcanic stratigraphy of large-volume silicic pyroclastic eruptions during Oligocene Afro-Arabian flood volcanism in Yemen, Bull. Volcanol., 68, 135–156, https://doi.org/10.1007/s00445-005-0428-4, 2005.

Plaziat, J.-C., Baltzer, F., Choukri, A., Conchon, O., Freytet, P., Orszag-Sperber, F., Raguideau, A., and Reyss, J.-L.: Quaternary marine and continental sedimentation in the northern Red Sea and Gulf of Suez (Egyptian coast): influences of rift tectonics, climatic changes and sea-level fluctuations, in: Sedimentation and Tectonics in Rift Basins Red Sea: Gulf of Aden, Springer Netherlands, 537–573, https://doi.org/10.1007/978-94-011-4930-3_29, 1998.

Prave, A. R., Bates, C. R., Donaldson, C. H., Toland, H., Condon, D. J., Mark, D., and Raub, T. D.: Geology and geochronology of the Tana Basin, Ethiopia: LIP volcanism, Super eruptions and Eocene-Oligocene environmental change, Earth Planet. Sc. Lett., 443, 1–8, https://doi.org/10.1016/j.epsl.2016.03.009, 2016.

Pusok, A. E. and Stegman, D. R.: The convergence history of India-Eurasia records multiple subduction dynamics processes, Sci. Adv., 6, eaaz8681, https://doi.org/10.1126/sciadv.aaz8681, 2020.

Qaysi, S., Liu, K. H., and Gao, S. S.: A Database of Shear-Wave Splitting Measurements for the Arabian Plate, Seismol. Res. Lett., 89, 2294–2298, https://doi.org/10.1785/0220180144, 2018.

Reilinger, R. and McClusky, S.: Nubia-Arabia-Eurasia plate motions and the dynamics of Mediterranean and Middle East tectonics, Geophys. J. Int., 186, 971–979, https://doi.org/10.1111/j.1365-246X.2011.05133.x, 2011.

Reilinger, R., McClusky, S., Vernant, P., Lawrence, S., Ergintav, S., Cakmak, R., Ozener, H., Kadirov, F., Guliev, I., Stepanyan, R., and Nadariya, M.: GPS constraints on continental deformation in the Africa-Arabia-Eurasia continental collision zone and implications for the dynamics of plate interactions, J. Geophys. Res.-Solid, 111, B05411, https://doi.org/10.1029/2005JB004051, 2006.

Richards, M. A., Duncan, R. A., and Courtillot, V. E.: Flood basalts and hot-spot tracks: Plume heads and tails, Science, 246, 103–107, https://doi.org/10.1126/science.246.4926.103, 1989.

Rime, V., Foubert, A., Ruch, J., and Kidane, T.: Tectonostratigraphic evolution and significance of the Afar Depression, Earth-Sci. Rev., 244, 104519, https://doi.org/10.1016/j.earscirev.2023.104519, 2023.

Roger, J., Platel, J. P., Cavelier, C., and Bourdillon-de-Grissac, C.: Données nouvelles sur la stratigraphie et l'histoire géologique du Dhofar (Sultanat d'Oman), Bull. Soc. Géol. Fr., 2, 256–277, 1989.

Rooney, T. O.: The Cenozoic magmatism of East-Africa: Part I – Flood basalts and pulsed magmatism, Lithos, 286–287, 264–301, https://doi.org/10.1016/j.lithos.2017.05.014, 2017.

Ruch, J., Keir, D., Passarelli, L., Di Giacomo, D., Ogubazghi, G., and Jónsson, S.: Revealing 60 years of Earthquake Swarms in the Southern Red Sea, Afar and the Gulf of Aden, Front. Earth Sci., 9, 690, https://doi.org/10.3389/feart.2021.664673, 2021.

Sandwell, D. T., Müller, R. D., Smith, W. H.F ., Garcia, E., and Francis, R.: New global marine gravity model from CryoSat-2 and Jason-1 reveals buried tectonic structure, Science, 346, 65–67, https://doi.org/10.1126/SCIENCE.1258213, 2014 (data

available at: https://topex.ucsd.edu/grav_outreach/, last access: 9 July 2024).

Schettino, A., Macchiavelli, C., Pierantoni, P. P., Zanoni, D., and Rasul, N.: Recent kinematics of the tectonic plates surrounding the Red Sea and Gulf of Aden, Geophys. J. Int., 207, 457–480, https://doi.org/10.1093/gji/ggw280, 2016.

Schettino, A., Macchiavelli, C., and Rasul, N. M. A.: Plate motions around the red sea since the early oligocene, in: Geological Setting, Palaeoenvironment and Archaeology of the Red Sea, Springer International Publishing, 203–220, https://doi.org/10.1007/978-3-319-99408-6_9, 2018.

Schult, A.: Palaeomagnetism of tertiary volcanic rocks from the Ethiopian southern plateau and the Danakil block, J. Geophys., 40, 203–212, 1974.

Sembroni, A., Faccenna, C., Becker, T. W., Molin, P., and Abebe, B.: Long-term, deep-mantle support of the Ethiopia-Yemen Plateau, Tectonics, 35, 469–488, https://doi.org/10.1002/2015TC004000, 2016.

Sengör, A. M. C. and Burke, K.: Relative timing of rifting and volcanism on Earth and its tectonic implications, Geophys. Res. Lett., 5, 419–421, https://doi.org/10.1029/GL005I006P00419, 1978.

Sobolev, S. V., Sobolev, A. V., Kuzmin, D. V., Krivolutskaya, N. A., Petrunin, A. G., Arndt, N. T., Radko, V. A., and Vasiliev, Y. R.: Linking mantle plumes, large igneous provinces and environmental catastrophes, Nature, 477, 312–316, https://doi.org/10.1038/nature10385, 2011.

Stamps, D. S., Flesch, L. M., Calais, E., and Ghosh, A.: Current kinematics and dynamics of Africa and the East African Rift System, J. Geophys. Res.-Solid, 119, 5161–5186, https://doi.org/10.1002/2013JB010717, 2014.

Stockli, D. F. and Bosworth, W. B.: Timing of extensional faulting along the magma-poor central and northern red sea rift margin-transition from regional extension to necking along a hyperextended rifted margin, in: Geological Setting, Palaeoenvironment and Archaeology of the Red Sea, Springer International Publishing, 81–111, https://doi.org/10.1007/978-3-319-99408-6_5, 2018.

Su, H. and Zhou, J.: Timing of Arabia-Eurasia collision: Constraints from restoration of crustal-scale cross-sections, J. Struct. Geol., 135, 104041, https://doi.org/10.1016/j.jsg.2020.104041, 2020.

Szymanski, E., Stockli, D. F., Johnson, P. R., and Hager, C.: Thermochronometric evidence for diffuse extension and two-phase rifting within the Central Arabian Margin of the Red Sea Rift, Tectonics, 35, 2863–2895, https://doi.org/10.1002/2016TC004336, 2016.

Tazieff, H. T., Varet, J., Barberi, F., and Giglia, G.: Tectonic significance of the Afar (or Danakil) depression, Nature, 235, 144–147, 1972.

Tesfaye, S., Harding, D. J., and Kusky, T. M.: Early continental breakup boundary and migration of the Afar triple junction, Ethiopia, Bull. Geol. Soc. Am., 115, 1053–1067, https://doi.org/10.1130/B25149.1, 2003.

van Hinsbergen, D. J. J., Steinberger, B., Doubrovine, P. V., and Gassmöller, R.: Acceleration and deceleration of India-Asia convergence since the Cretaceous: Roles of mantle plumes and continental collision, J. Geophys. Res.-Solid, 116, 6101, https://doi.org/10.1029/2010JB008051, 2011.

van Hinsbergen, D. J., Steinberger, B., Guilmette, C., Maffione, M., Gürer, D., Peters, K., Plunder, A., McPhee, P. J., Gaina, C., Advokaat, E. L., and Vissers, R. L.: A record of plume-induced plate rotation triggering subduction initiation, Nat. Geosci., 14, 626–630, https://doi.org/10.1038/s41561-021-00780-7, 2021.

Varet, J.: Geological map of Central and Southern Afar – (Ethiopia and djibouti republic), https://geocatalogue.africamuseum.be/geonetwork/srv/api/records/BE-RMCA-EARTHS-000649 (last access: 18 June 2024), 1975.

Varet, J.: Geology of Afar (East Africa), Springer, 1–249, ISBN 9783319608631, 2018.

Viltres, R., Jónsson, S., Ruch, J., Doubre, C., Reilinger, R., Floyd, M., and Ogubazghi, G.: Kinematics and deformation of the southern Red Sea region from GPS observations, Geophys. J. Int., 221, 2143–2154, https://doi.org/10.1093/gji/ggaa109, 2020.

Viltres, R., Jónsson, S., Alothman, A. O., Liu, S., Leroy, S., Masson, F., Doubre, C., and Reilinger, R.: Present-Day Motion of the Arabian Plate, Tectonics, 41, e2021TC007013, https://doi.org/10.1029/2021TC007013, 2022.

Watchorn, F., Nichols, G. J., and Bosence, D. W. J.: Rift-related sedimentation and stratigraphy, southern Yemen (Gulf of Aden), in: Sedimentation and Tectonics in Rift Basins Red Sea: Gulf of Aden, Springer Netherlands, 165–189, https://doi.org/10.1007/978-94-011-4930-3_11, 1998.

Wescott, W. A., Wigger, S. T., Stone, D. M., and Morley, C. K.: Geology and Geophysics of the Lotikipi Plain, in: Geoscience of Rift Systems – Evolution of East Africa, AAPG Stud. Geol., 44, 55–65, https://doi.org/10.1306/St44623C3, 1999.

White, R. and McKenzie, D.: Magmatism at rift zones: the generation of volcanic continental margins and flood basalts, J. Geophys. Res., 94, 7685–7729, https://doi.org/10.1029/JB094iB06p07685, 1989.

White, R. S. and McKenzie, D.: Mantle plumes and flood basalts, J. Geophys. Res., 100, 543–560, https://doi.org/10.1029/95jb01585, 1995.

Will, T. M. and Frimmel, H. E.: Where does a continent prefer to break up? Some lessons from the South Atlantic margins, Gondwana Res., 53, 9–19, https://doi.org/10.1016/j.gr.2017.04.014, 2018.

Wilson, J. T.: A possible origin of the Hawaiian Islands, Can. J. Phys., 41, 863–870, https://doi.org/10.1139/P63-094, 1963.

Wolfenden, E., Ebinger, C., Yirgu, G., Deino, A., and Ayalew, D.: Evolution of the northern Main Ethiopian rift: Birth of a triple junction, Earth Planet. Sc. Lett., 224, 213–228, https://doi.org/10.1016/j.epsl.2004.04.022, 2004.

Zingerle, P., Pail, R., Gruber, T., and Oikonomidou, X.: The experimental gravity field model XGM2019e, GFZ Data Serv. [data set], https://doi.org/10.5880/ICGEM.2019.007, 2019.

Zingerle, P., Pail, R., Gruber, T., and Oikonomidou, X.: The combined global gravity field model XGM2019e, J. Geod., 94, 66, https://doi.org/10.1007/S00190-020-01398-0, 2020.

Zwaan, F., Corti, G., Keir, D., and Sani, F.: A review of tectonic models for the rifted margin of Afar: Implications for continental break-up and passive margin formation, J. Afr. Earth Sci., 164, 103649, https://doi.org/10.1016/j.jafrearsci.2019.103649, 2020a.

Zwaan, F., Corti, G., Sani, F., Keir, D., Muluneh, A. A., Illsley-Kemp, F., and Papini, M.: Structural Analysis of the Western Afar Margin, East Africa: Evidence for Multiphase Rotational Rifting, Tectonics, 39, e2019TC006043, https://doi.org/10.1029/2019TC006043, 2020b.